Search for New Physics with b→sll decays @ LHCb

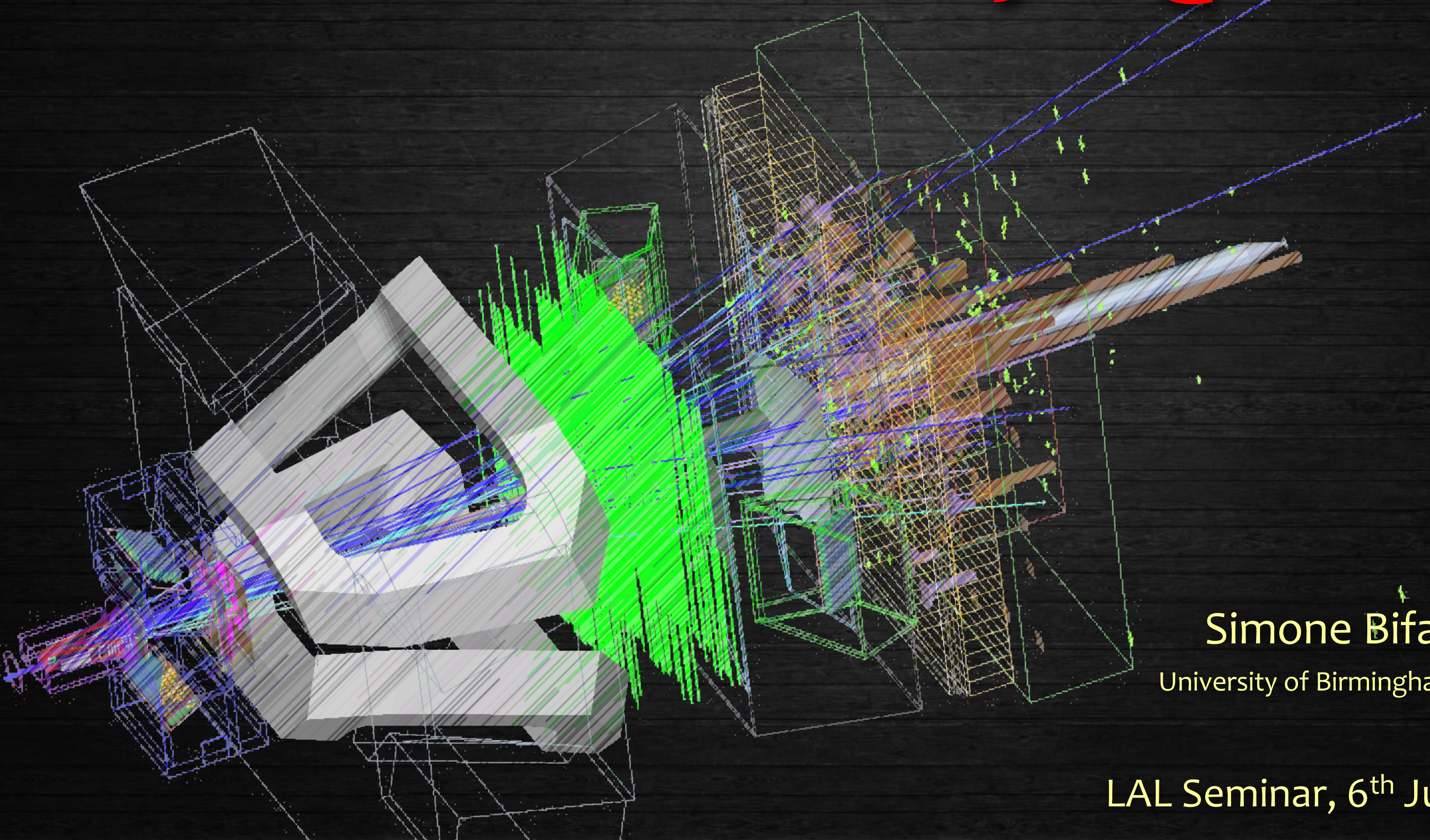

Simone Bifani
University of Birmingham (UK)

LAL Seminar, 6th June 2017

A Forward Spectrometer

- Optimized for beauty and charm physics at large pseudorapidity ($2<\eta<5$)
  - **Trigger**: >95% (60-70%) efficient for muons (electrons)
  - **Tracking**: σ_p/p 0.4%–0.6% (p from 5 to 100 GeV), $\sigma_{IP} < 20\ \mu m$
  - **Calorimeter**: $\sigma_E/E \sim 10\% / \sqrt{E} \oplus 1\%$
  - **PID**: ~97% μ,e ID for 1–3% $\pi\rightarrow\mu$,e misID

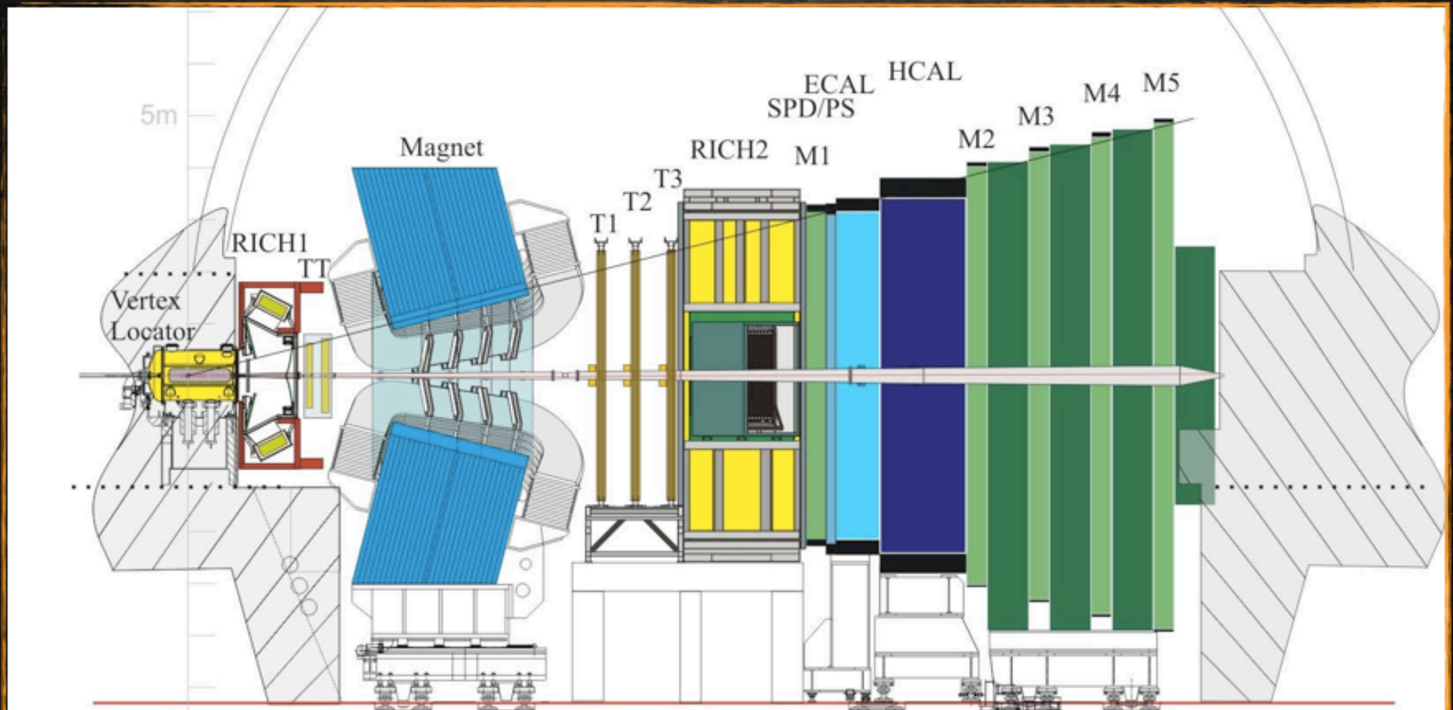

JINST 3 (2008) S08005 Int.J.Mod.Phys. A30 (2015)

Datasets

› Analyses presented today based on the full **Run-I** dataset

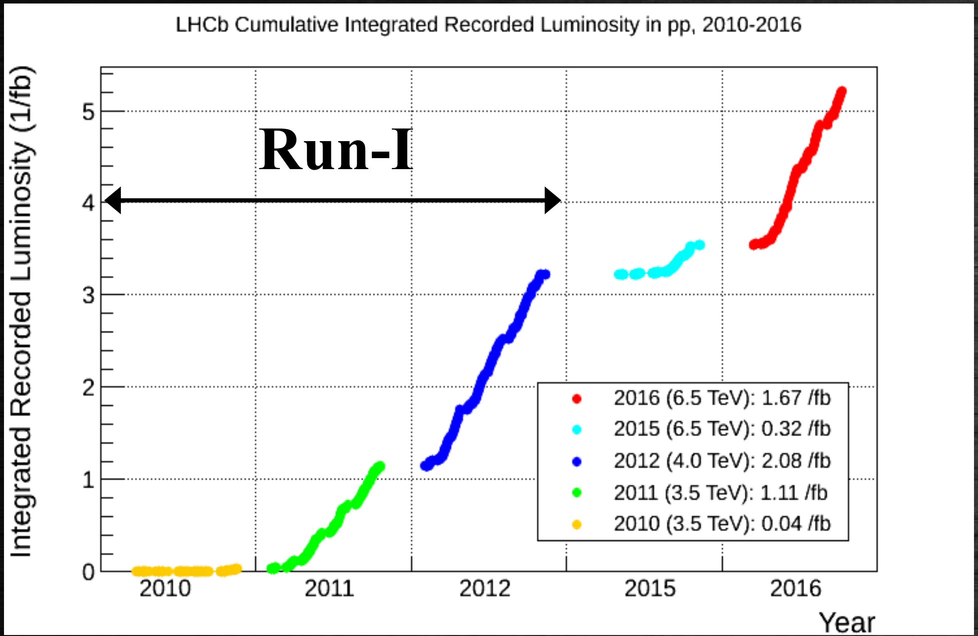

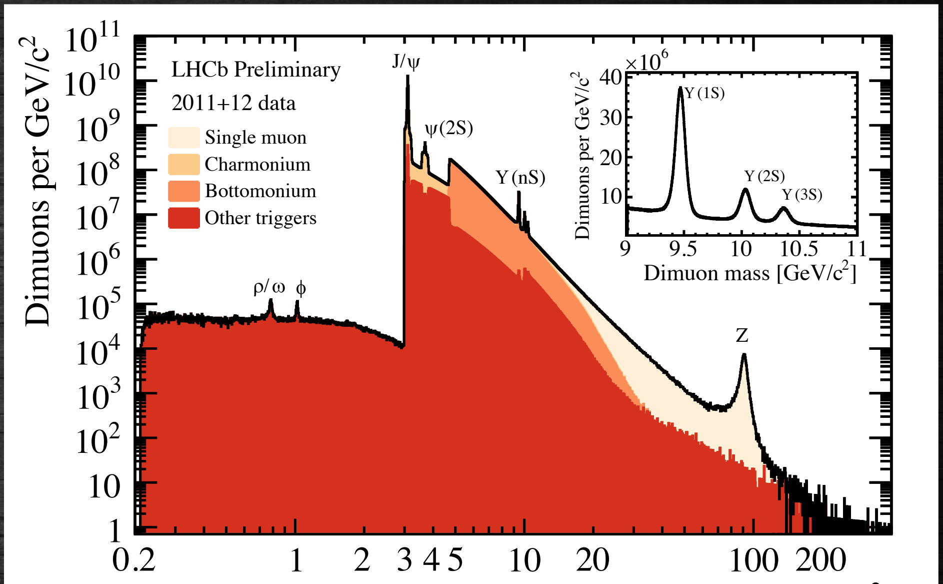

[LHCB-CONF-2016-005](#)

› Due to luminosity levelling, same running conditions throughout fills

Why Rare b-Decays?

- $b \to sll$ decays proceed via **FCNC transitions** that only occur at loop order (or beyond) in the SM

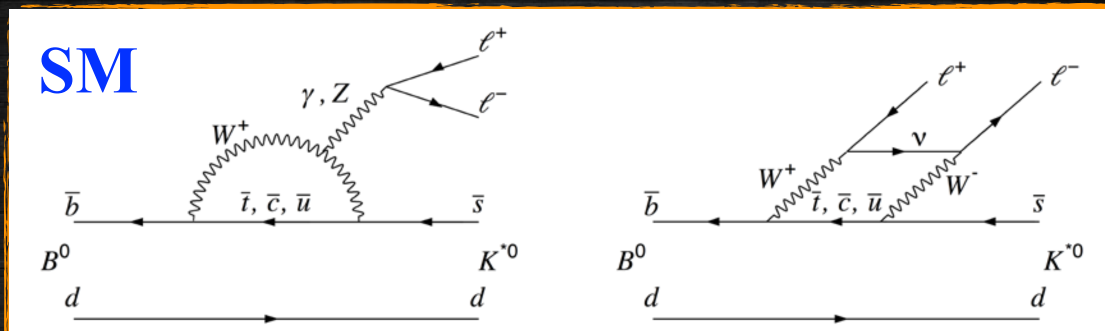

- New particles can for example contribute to loop or tree level diagrams by enhancing/suppressing decay rates, introducing new sources of CP violation or modifying the angular distribution of the final-state particles

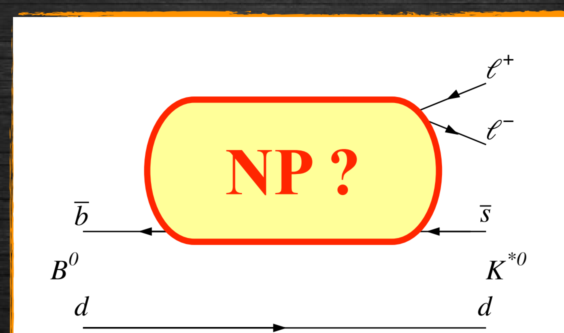

- **Rare b decays place strong constraints on many New Physics models by probing energy scales higher than direct searches**

Theoretical Framework – I

› FCNC **effective Hamiltonian** described by Operator Product Expansion

$$H_{eff} = -\frac{4G_F}{\sqrt{2}} V_{tb} V_{ts}^* \sum_i [\underbrace{\mathcal{C}_i(\mu)\mathcal{O}_i(\mu)}_{\text{left-handed part}} + \underbrace{\mathcal{C}_i'(\mu)\mathcal{O}_i'(\mu)}_{\substack{\text{right-handed part}\\ \text{suppressed in SM}}}]$$

i=1, 2	Tree
i=3-6, 8	Gluon penguin
i=7	Photon penguin
i=9, 10	Electroweak penguin
i=S	Higgs (scalar) penguin
i=P	Pseudoscalar penguin

› C_i (**Wilson coefficients**): perturbative, short-distance physics, sensitive to $E>\Lambda_{EW}$

› O_i (**Operators**): non-perturbative QCD, long distance physics, depends on hadronic form factors

0.2GeV……	4GeV……	80GeV……	~ 100 TeV ?
Λ_{QCD}	Λ_b	Λ_{EW}	Λ_{NP}
(non-perturbative regime)	(b mass)	(W mass)	(new physics scale)

Theoretical Framework – II

- **New Physics** can
  - » alter the SM operator contributions (Wilson coefficients)
  - » enter through new operators (right-handed O_i', $O_{S,P}$)

- Different q² regions probe different processes

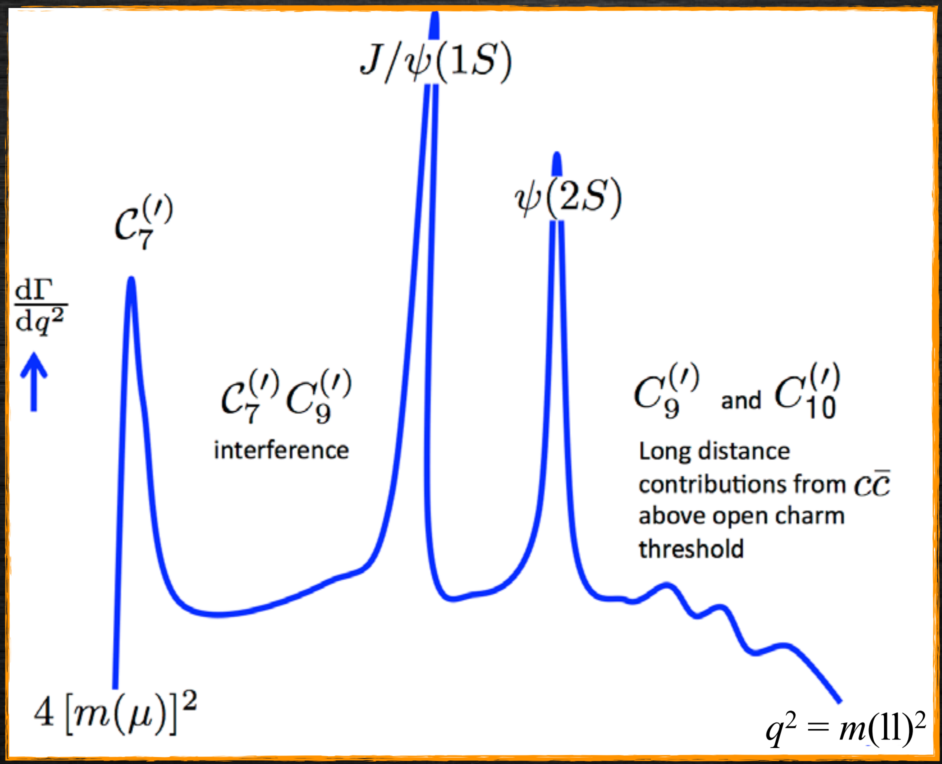

Shopping List

› **New Physics** searches in three main areas

1. **Differential branching fractions** of $B^0 \to K^{(*)0}\mu\mu$, $B^+ \to K^{(*)+}\mu\mu$, $B_s \to \phi\mu\mu$, $B^+ \to \pi^+\mu\mu$ and $\Lambda_b \to \Lambda\mu\mu$
   » Presence of hadronic uncertainties in theory predictions

2. **Angular analyses** of $B \to K^{(*)}\mu\mu$, $B_s \to \phi\mu\mu$, $B^0 \to K^{*0}ee$ and $\Lambda_b \to \Lambda\mu\mu$
   » Define observables with smaller theory uncertainties

3. **Test of Lepton Universality** in $B^+ \to K^+ll$ and $B^0 \to K^{*0}ll$
   » Cancellation of hadronic uncertainties in theory predictions

Differential Branching Fractions

› Results **consistently lower than SM predictions**

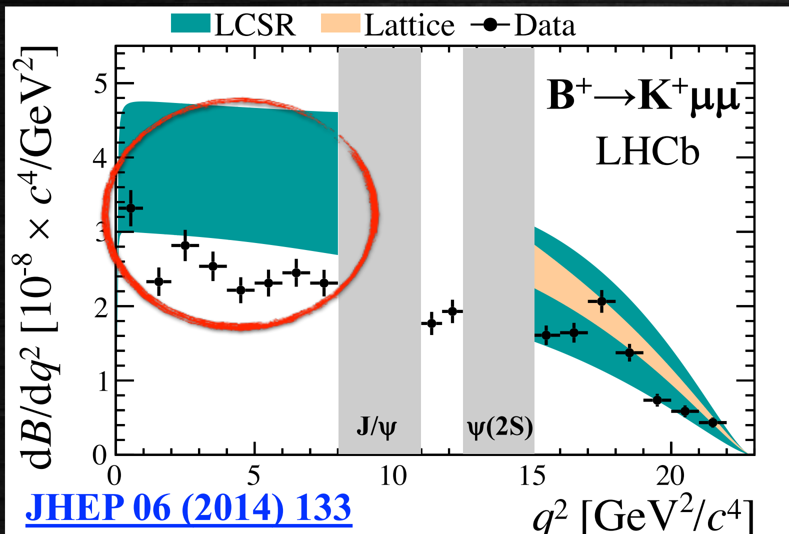

JHEP 06 (2014) 133

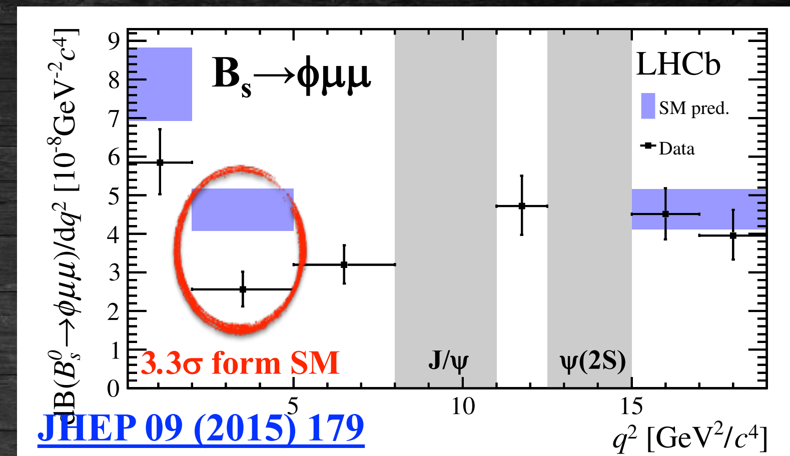

JHEP 09 (2015) 179

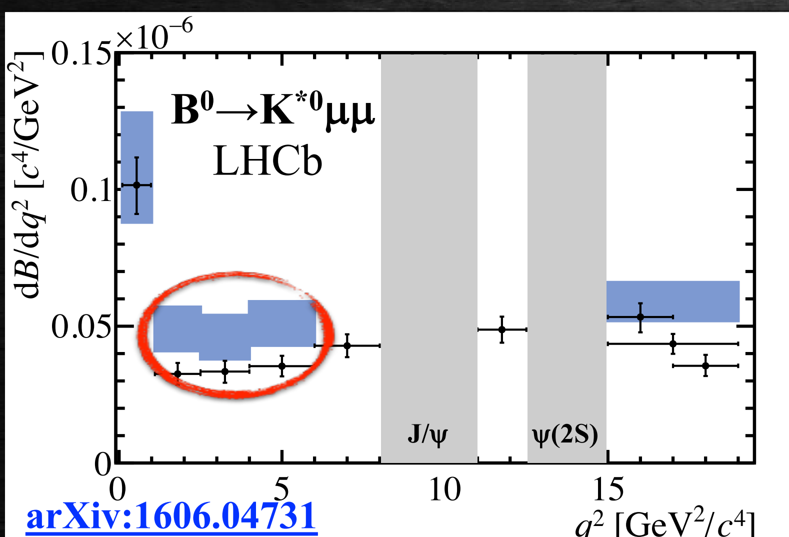

arXiv:1606.04731

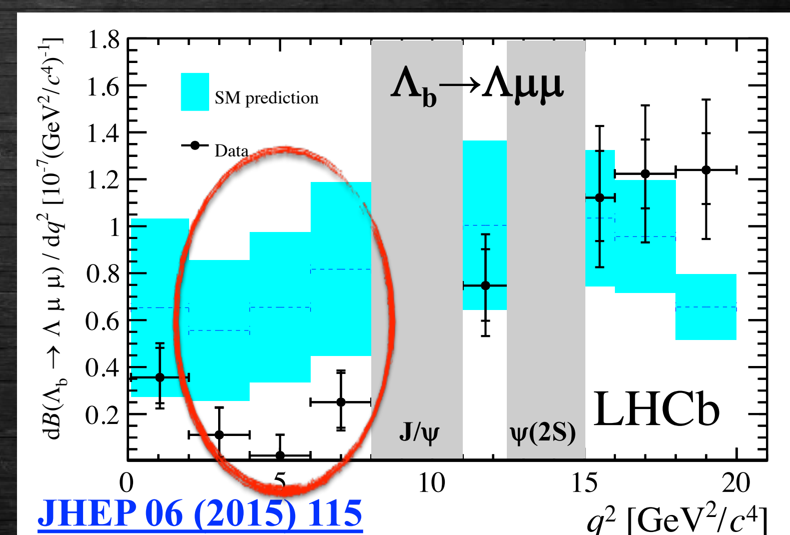

JHEP 06 (2015) 115

Angular Analyses

- First **full angular analysis** of $B^0 \to K^{*0}\mu\mu$: measured all CP-averaged angular terms and CP-asymmetries
- Can construct **less form-factor dependent ratios of observables**

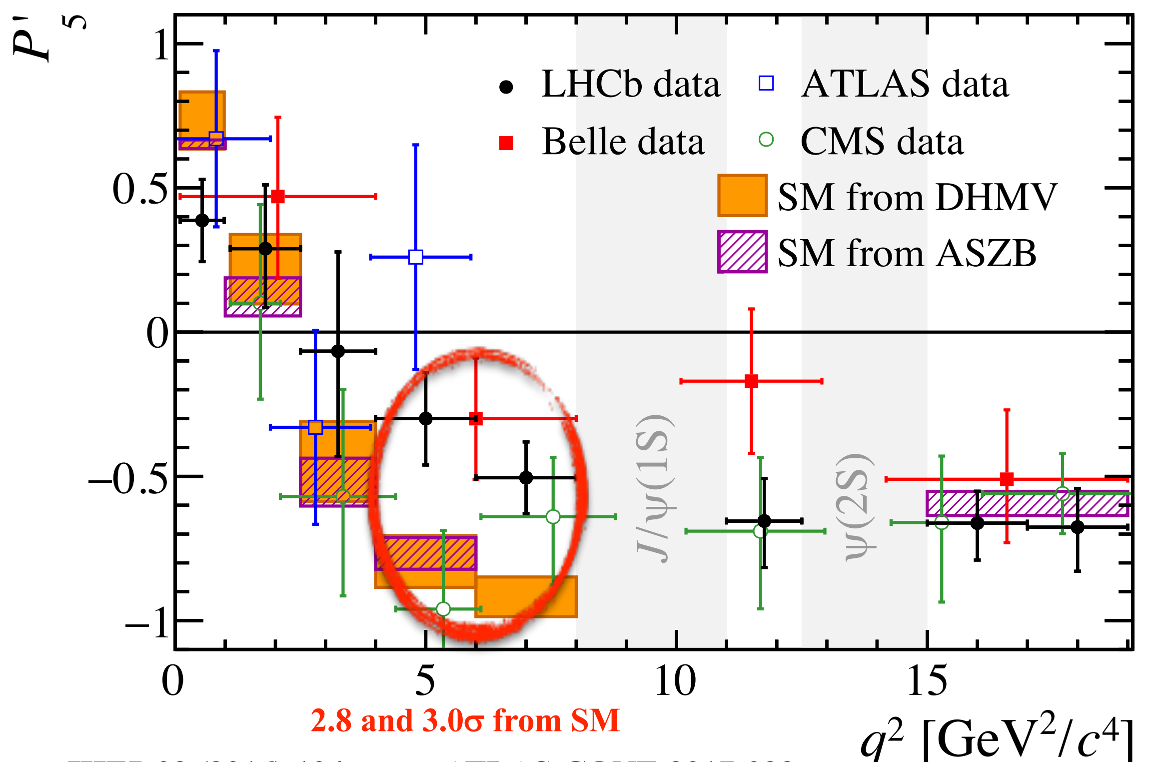

- JHEP 02 (2016) 104
- PRL 118 (2017)
- ATLAS-CONF-2017-023
- CMS-PAS-BPH-15-008

Test of LU – R_K

› LHCb tested Lepton Flavour Universality using **$B^+ \to K^+ ll$** decays and observed a **tension with the SM at 2.6σ**

$$\mathcal{R}_K = \frac{\mathcal{B}(B^+ \to K^+ \mu^+ \mu^-)}{\mathcal{B}(B^+ \to K^+ J/\psi(\to \mu^+ \mu^-))} \Bigg/ \frac{\mathcal{B}(B^+ \to K^+ e^+ e^-)}{\mathcal{B}(B^+ \to K^+ J/\psi(\to e^+ e^-))}$$

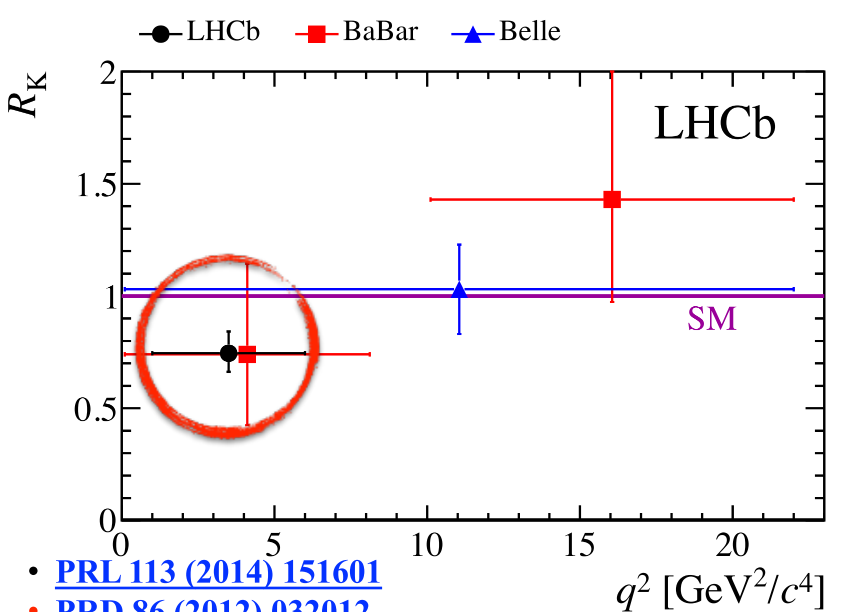

- PRL 113 (2014) 151601
- PRD 86 (2012) 032012
- PRL 103 (2009) 171801

› Consistent with observed BR($B^+ \to K^+ \mu\mu$) if NP does not couple to electrons

› **Observation of LU violation would be a clear sign of NP**

Test of LU – $R_{K^{*0}}$

arXiv:1705.05802

- Test of LFU with **$B^0 \to K^{*0}\mu\mu$** and **$B^0 \to K^{*0}ee$**

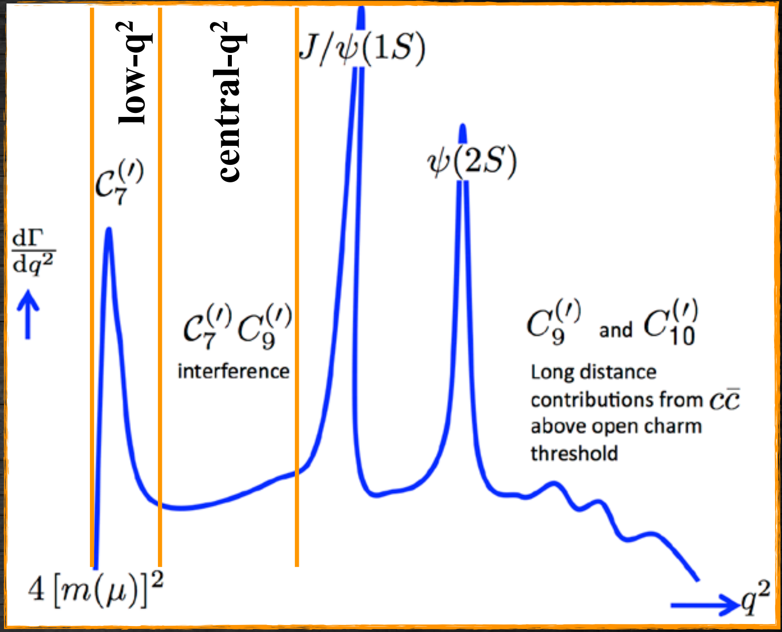

- **Two regions of q^2**
  - Low [0.045-1.1] GeV²/c⁴
  - Central [1.1-6.0] GeV²/c⁴

- Measured relative to **$B^0 \to K^{*0}J/\psi(ll)$** in order to reduce systematics
- K^{*0} reconstructed as **$K^+\pi^-$** within 100MeV from the $K^*(892)^0$
- **Blind analysis** to avoid experimental biases
- Extremely challenging due to significant differences in the way muons and electrons "interact" with the detector (bremsstrahlung and trigger)

Bremsstrahlung – I

› Electrons emit a large amount of bremsstrahlung that results in degraded momentum and mass resolutions

› **Two types of bremsstrahlung**

» **Downstream of the magnet**

- photon energy in the same calorimeter cell as the electron
- momentum correctly measured

» **Upstream of the magnet**

- photon energy in different calorimeter cells than electron
- momentum evaluated after bremsstrahlung

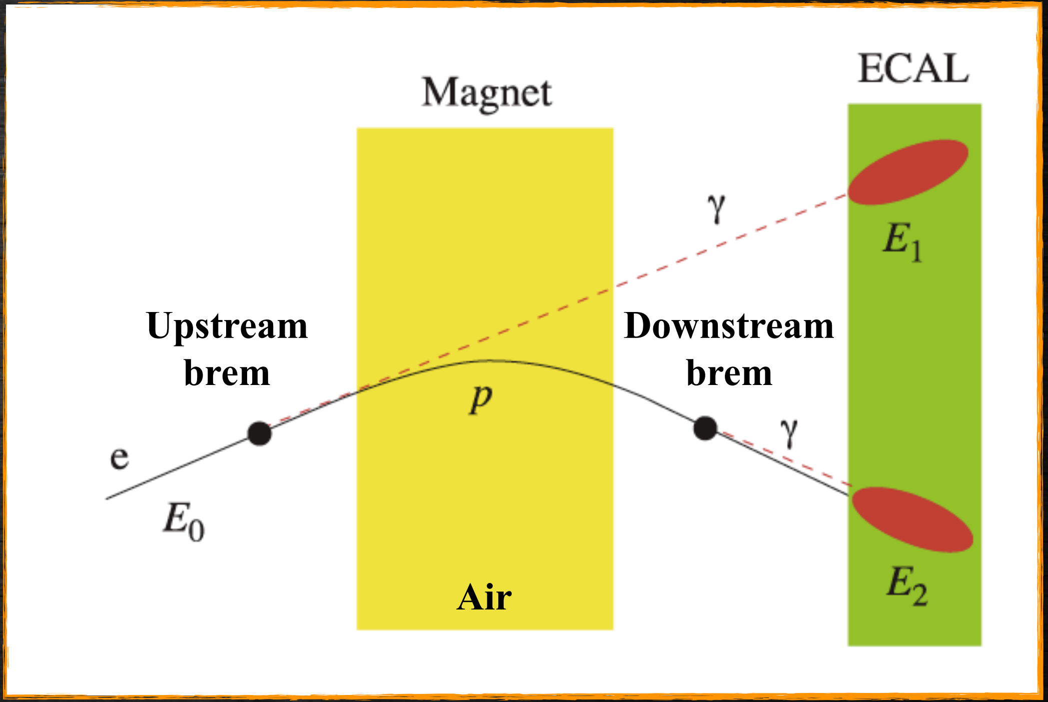

Event Anatomy

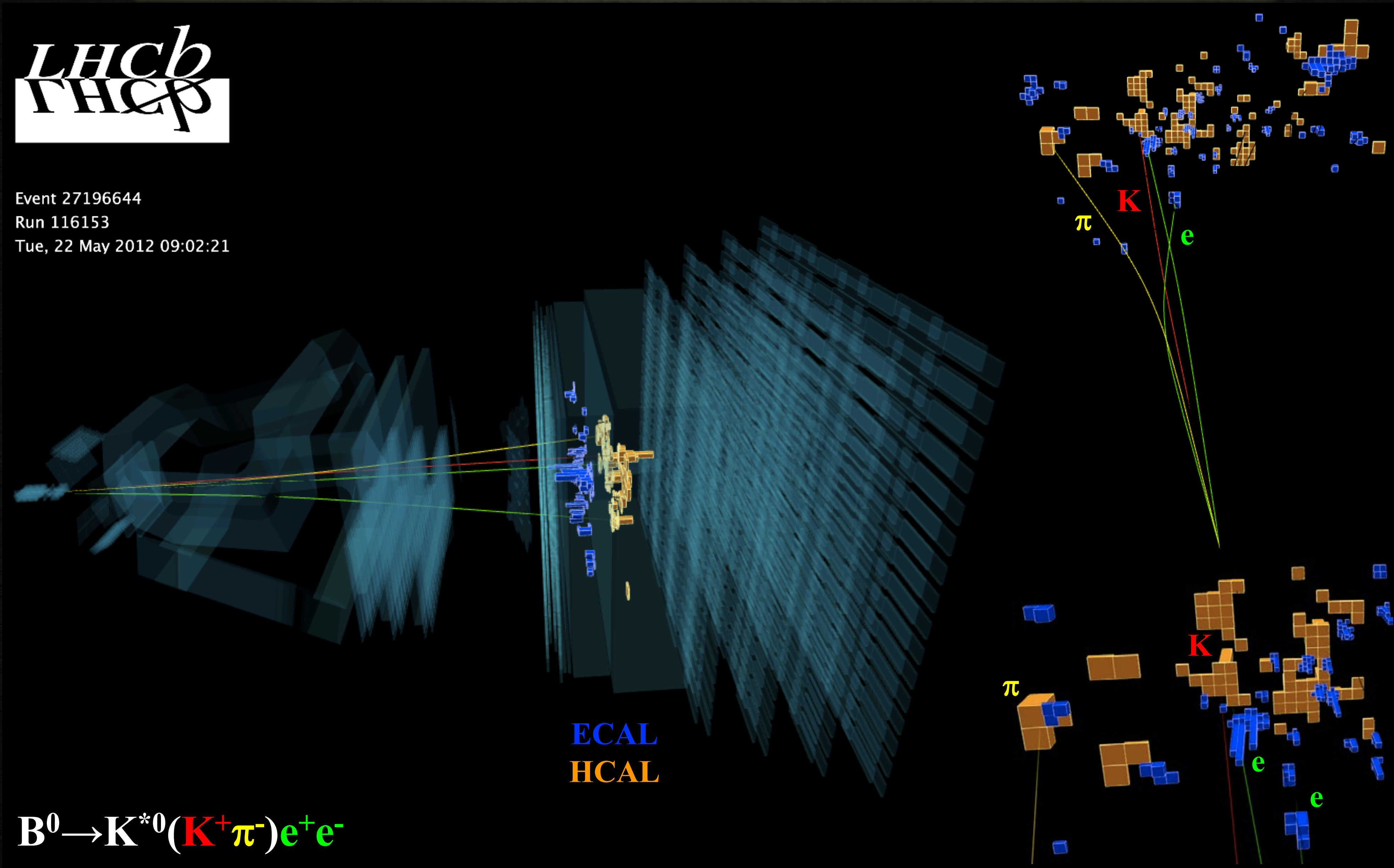

Bremsstrahlung – II

- A **recovery procedure** is in place to improve the momentum reconstruction
- Events categorised depending on the number of recovered brem-clusters
- Incomplete recovery due to the calorimeter acceptance, the energy threshold (E_T > 75 MeV), and the presence of energy deposits mistaken as brem-clusters

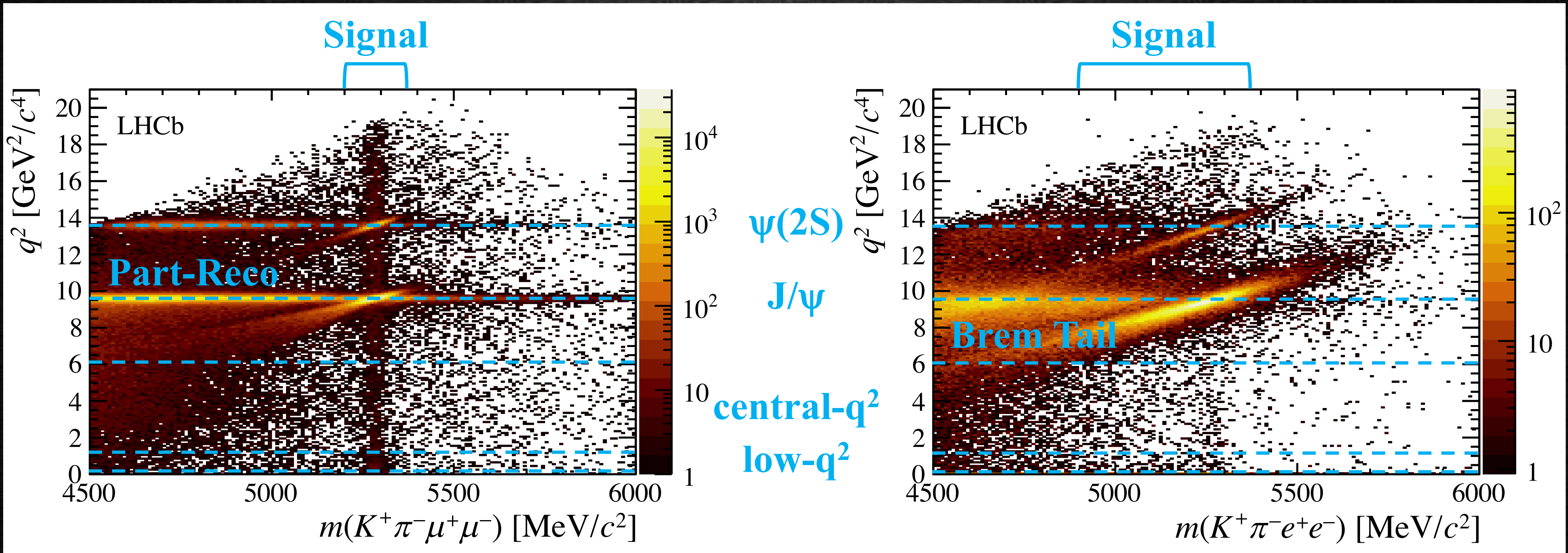

- Incomplete recovery causes the reconstructed B mass to shift towards lower values and events to migrate in and out of the q^2 regions

arXiv:1705.05802

Trigger

› Trigger system split in hardware (L0) and software (HLT) stages

› Due to higher occupancy of the calorimeters compared to the muon stations, hardware thresholds on the electron E_T are higher than on the muon p_T (**L0 Muon**, $p_T > 1.5\text{-}1.8$ GeV)

› To partially mitigate this effect, **3 exclusive trigger categories** are defined for the electron sample

» **L0 Electron**: electron hardware trigger fired by clusters associated to at least one of the two electrons ($E_T > 2.5\text{-}3.0$ GeV)

» **L0 Hadron**: hadron hardware trigger fired by clusters associated to at least one of the K^{*0} decay products ($E_T > 3.5$ GeV)

» **L0 TIS**: any hardware trigger fired by particles in the event not associated to the signal candidate

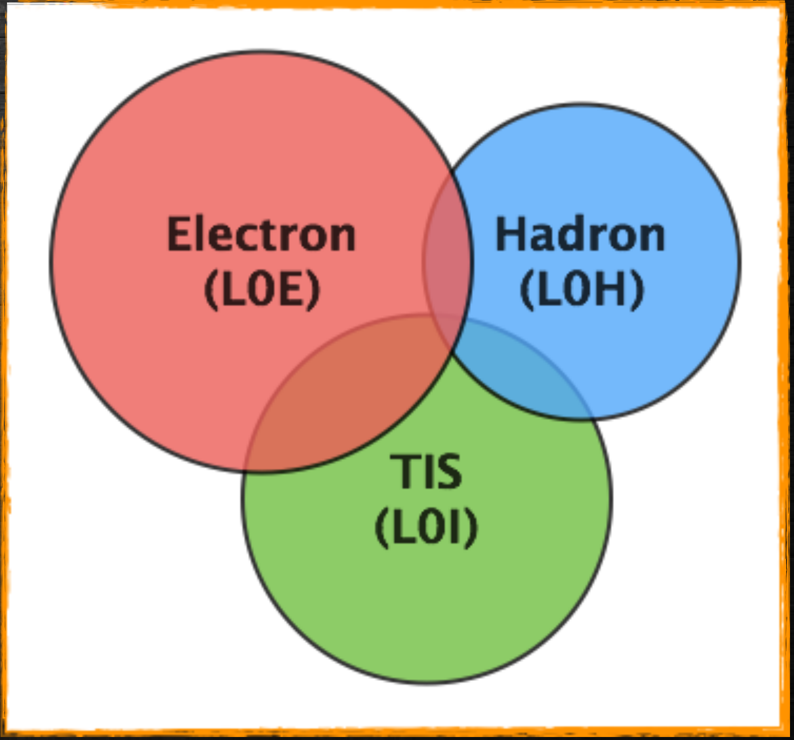

Strategy

› $R_{K^{*0}}$ determined as double ratio to reduce systematic effects

$$\mathcal{R}_{K^{*0}} = \frac{\mathcal{B}(B^0 \to K^{*0}\mu^+\mu^-)}{\mathcal{B}(B^0 \to K^{*0}J/\psi(\to \mu^+\mu^-))} \Big/ \frac{\mathcal{B}(B^0 \to K^{*0}e^+e^-)}{\mathcal{B}(B^0 \to K^{*0}J/\psi(\to e^+e^-))}$$

› Selection as similar as possible between μμ and ee

» Pre-selection requirements on quality of the candidates

» Cuts to remove the peaking backgrounds

» Particle identification to further reduce the background

» Multivariate classifier to reject the combinatorial background

» Kinematic requirements to reduce the partially-reconstructed backgrounds

» Multiple candidates randomly rejected (1-2%)

› Efficiencies

» Determined using simulation, which is tuned with data

» Final-state radiation corrected for with PHOTOS
(residual QED effects O(%) arXiv:1605.07633)

Corrections to Simulation

› Four-step procedure largely based on tag-and-probe technique

1. **Particle identification**
   » PID response of each particle species tuned using dedicated calibration samples

2. **Generator**
   » Event multiplicity and B^0 kinematics matched to data using $B^0 \rightarrow K^{*0} J/\psi(\mu\mu)$ decay

3. **Trigger**
   » Hardware and software trigger responses tuned using $B^0 \rightarrow K^{*0} J/\psi(ll)$ decays

4. **Data/MC differences**
   » Residual discrepancies in variables entering the MVA reduced using $B^0 \rightarrow K^{*0} J/\psi(ll)$ decays

› After tuning, very good data/MC agreement in all key observables

Fit Procedure

- Fit signal MC to extract initial parameters
- Simultaneous fit to resonant and non-resonant modes
- Electron data split in three trigger categories

- **Signal**
  - $\mu\mu$ — Hypatia [NIM A, 764, 150 (2014)]
  - ee — Crystal-Ball (Crystal-Ball and Gaussian)
  - Free parameters — mass shift and width scale

- **Backgrounds**
  - **Combinatorial** — exponential
  - $\overline{\Lambda}_b \to K\bar{p}J/\psi(ll)$ — simulation & data, constrained using muons
  - $\overline{B}_s \to K^{*0}J/\psi(ll)$ — same as signal but shifted by m_{Bs}-m_{B0}, constrained using muons
  - (Λ_b and B_s backgrounds: $B^0 \to K^{*0}J/\psi$ only)
  - $B^0 \to K^{*0}J/\psi$ Leakage — simulation, yield constrained using data
  - **Part-Reco** — simulation & data
  - (Leakage and Part-Reco: $B^0 \to K^{*0}ee$ only)

Part-Reco Background – I

- Partially-reconstructed backgrounds arise from decays involving **higher K resonances** with one or more decay products in addition to a Kπ pair that are not reconstructed
- Large variety of decays, most abundant due to **$B\rightarrow K_1(1270)ee$** and **$B\rightarrow K_2^*(1430)ee$**

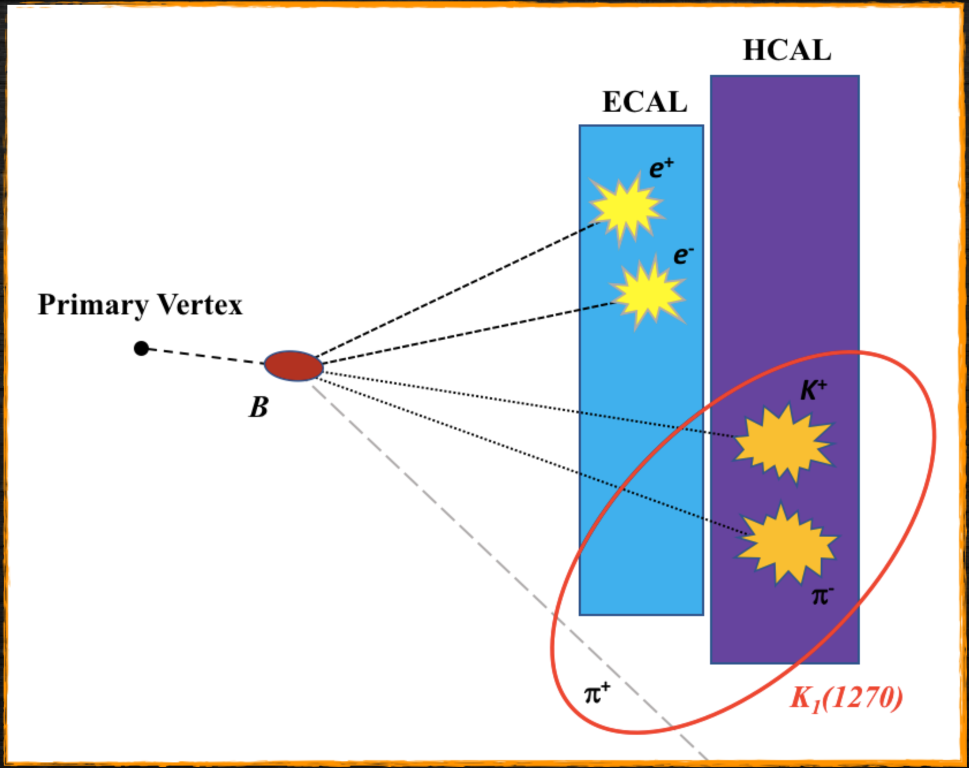

Part-Reco Background – II

› Modelled using two independent methods

» Create a K_1+K_2 cocktail from simulation and use $B \to XJ/\psi(ee)$ data to determine their relative fraction

» Re-weight $B^+ \to K^+\pi^+\pi^-ee$ simulated events using background subtracted $B^+ \to K^+\pi^+\pi^-\mu\mu$ data

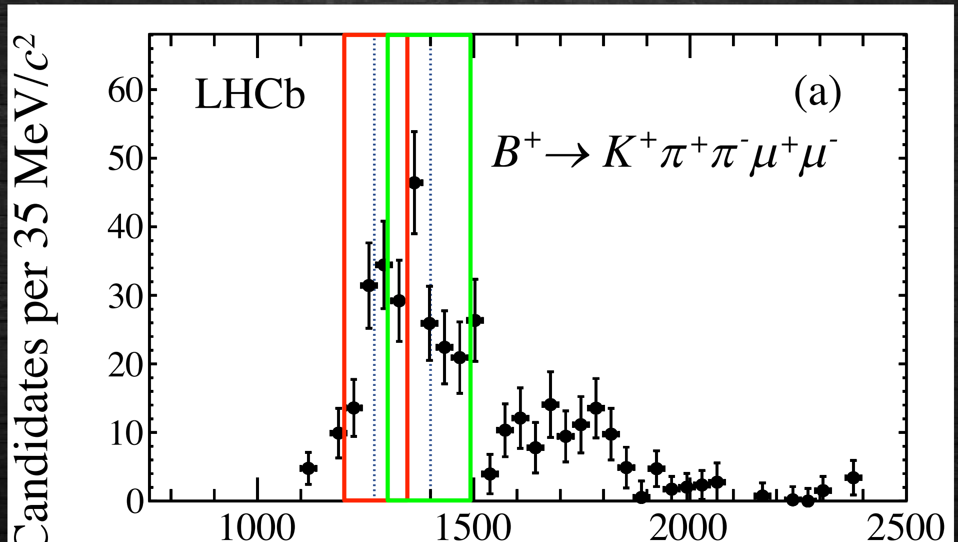

JHEP 10 (2014) 064

Fit Results

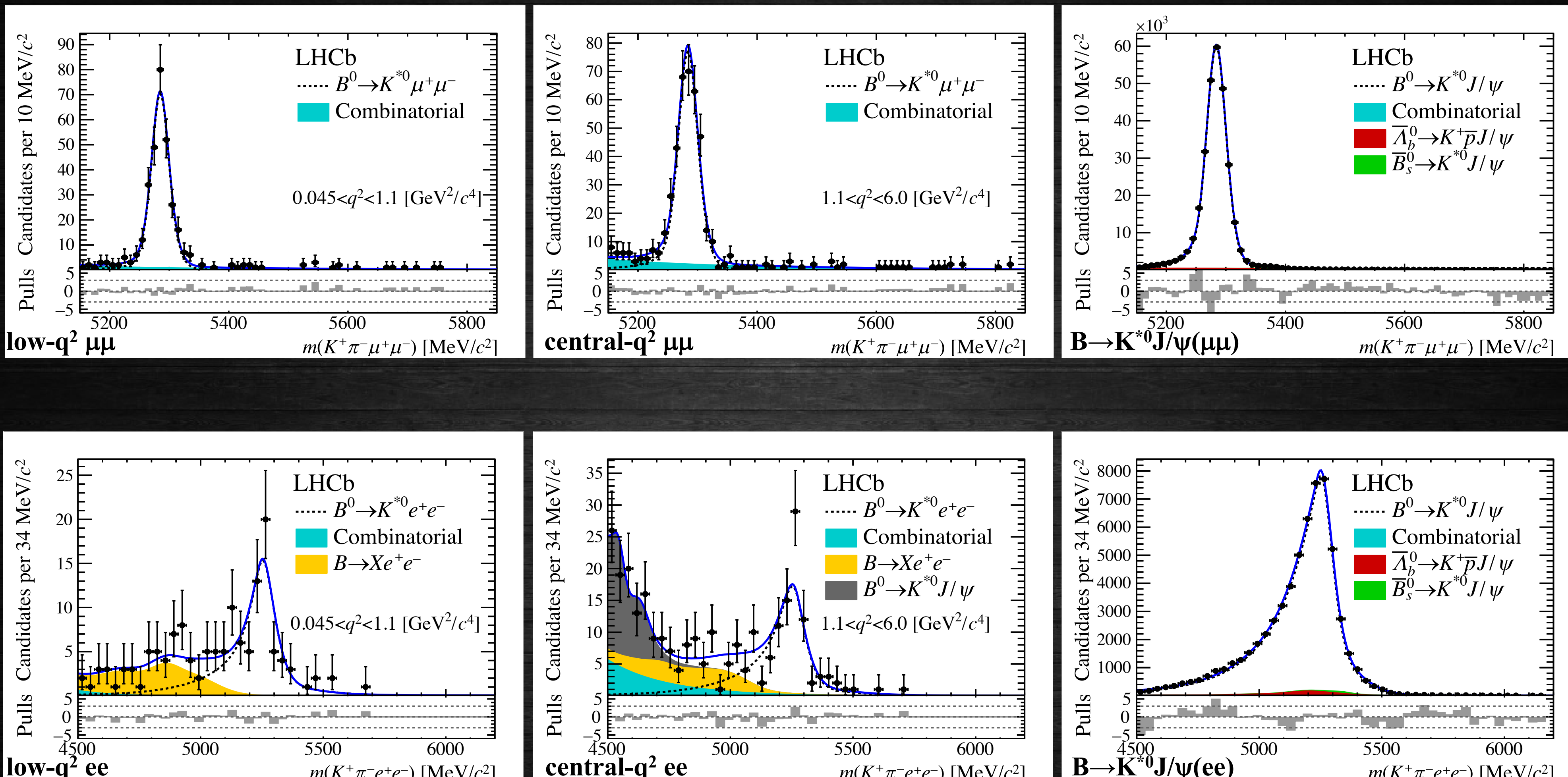

› In total, about 290 (90) and 350 (110) $B^0 \to K^{*0}\mu\mu$ ($B^0 \to K^{*0}ee$) candidates at low- and central-q^2, respectively

arXiv:1705.05802

Cross-Checks – I

› **Control of the absolute scale of the efficiencies** tested via the ratio

$$r_{J/\psi} = \frac{\mathcal{B}(B^0 \to K^{*0} J/\psi(\to \mu^+\mu^-))}{\mathcal{B}(B^0 \to K^{*0} J/\psi(\to e^+e^-))} = 1.043 \pm 0.006 \pm 0.045$$

compatible with unity and independent of the decay kinematics and event multiplicity

› **Further checks** performed by measuring the ratios

$$\mathcal{R}_{\psi(2S)} = \frac{\mathcal{B}(B^0 \to K^{*0} \psi(2S)(\to \mu^+\mu^-))}{\mathcal{B}(B^0 \to K^{*0} J/\psi(\to \mu^+\mu^-))} \Bigg/ \frac{\mathcal{B}(B^0 \to K^{*0} \psi(2S)(\to e^+e^-))}{\mathcal{B}(B^0 \to K^{*0} J/\psi(\to e^+e^-))}$$

$$r_{\gamma} = \frac{\mathcal{B}(B^0 \to K^{*0} \gamma(\to e^+e^-))}{\mathcal{B}(B^0 \to K^{*0} J/\psi(\to e^+e^-))}$$

compatible with the expectations

› **BR($B^0 \to K^{*0}\mu\mu$)** in good agreement with [arXiv:1606.04731]

› Relative population of **bremsstrahlung categories** consistent between data and simulation

› When **corrections to simulations** are not accounted for, the efficiency ratio changes by less than 5%

arXiv:1705.05802

Cross-Checks – II

› The sPlot technique is used to statistically subtract the background from the selected data [NIM A555, 356-369 (2005)]

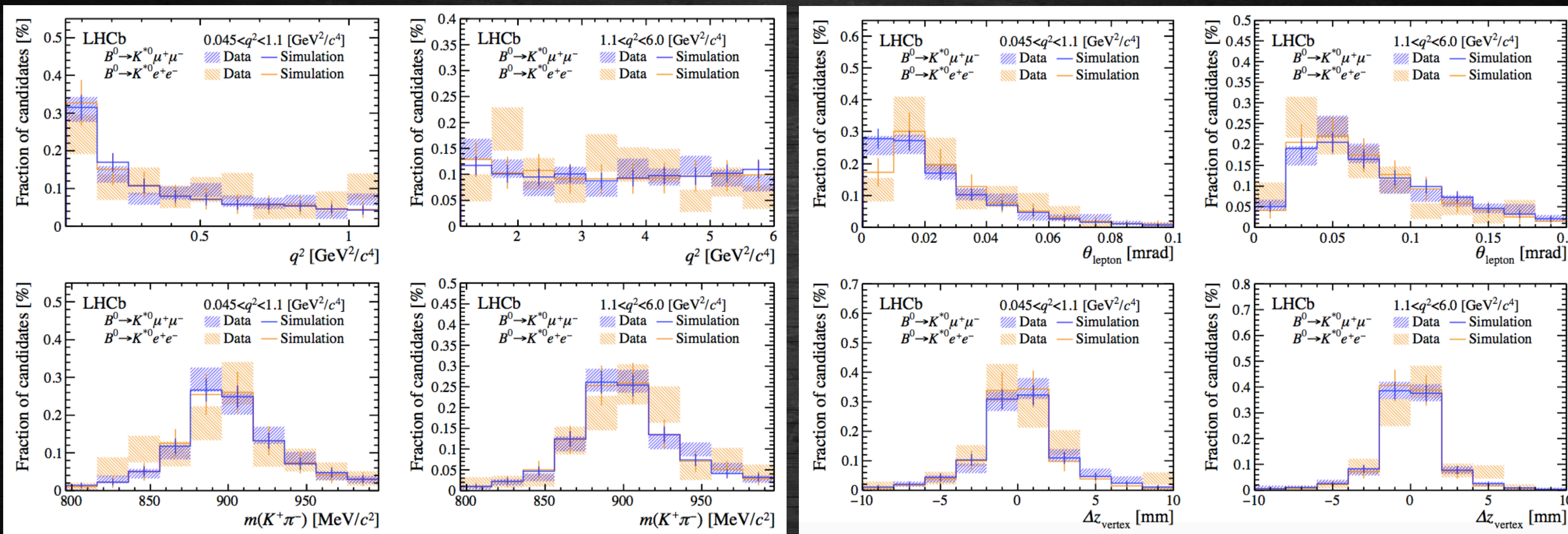

› A good agreement is observed in both q² regions between muons and electrons, data and simulation

arXiv:1705.05802

Systematics – I

- $R_{K^{*0}}$ **determined as a double ratio**
  - » Many experimental systematic effects cancel
  - » Statistically dominated (~15%)

arXiv:1705.05802

	$\Delta R_{K^{*0}}/R_{K^{*0}}$ [%]					
	low-q^2			central-q^2		
Trigger category	L0E	L0H	L0I	L0E	L0H	L0I
Corrections to simulation	2.5	4.8	3.9	2.2	4.2	3.4
Trigger	0.1	1.2	0.1	0.2	0.8	0.2
PID	0.2	0.4	0.3	0.2	1.0	0.5
Kinematic selection	2.1	2.1	2.1	2.1	2.1	2.1
Residual background	–	–	–	5.0	5.0	5.0
Mass fits	1.4	2.1	2.5	2.0	0.9	1.0
Bin migration	1.0	1.0	1.0	1.6	1.6	1.6
$r_{J/\psi}$ ratio	1.6	1.4	1.7	0.7	2.1	0.7
Total	4.0	6.1	5.5	6.4	7.5	6.7

- Total systematic uncertainty of 4-6% and 6-8% at low- and central-q^2

Systematics – II

- **Corrections to simulation**: besides the uncertainty due to the size of the samples, an additional systematic is determined using different parameterisations of the corrections
- **Kinematic selection**: a systematic uncertainty for Data/MC differences in the description of the bremsstrahlung tail and the MVA classifier is determined by comparing simulation and background subtracted $B^0 \to K^{*0} J/\psi(ll)$ data
- **Residual background**: both data and simulation are used to assess a systematic uncertainty for residual background contamination due to $B^0 \to K^{*0} J/\psi(ee)$ events with a $K \leftrightarrow e$ or $\pi \leftrightarrow e$ swap

arXiv:1705.05802

	$\Delta R_{K^{*0}}/R_{K^{*0}}$ [%]					
	low-q^2			central-q^2		
Trigger category	L0E	L0H	L0I	L0E	L0H	L0I
Corrections to simulation	2.5	4.8	3.9	2.2	4.2	3.4
Trigger	0.1	1.2	0.1	0.2	0.8	0.2
PID	0.2	0.4	0.3	0.2	1.0	0.5
Kinematic selection	2.1	2.1	2.1	2.1	2.1	2.1
Residual background	–	–	–	5.0	5.0	5.0
Mass fits	1.4	2.1	2.5	2.0	0.9	1.0
Bin migration	1.0	1.0	1.0	1.6	1.6	1.6
$r_{J/\psi}$ ratio	1.6	1.4	1.7	0.7	2.1	0.7
Total	4.0	6.1	5.5	6.4	7.5	6.7

Results – I

$$R_{K^{*0}} = \begin{cases} 0.66 \,{}^{+\,0.11}_{-\,0.07}\,(\text{stat}) \pm 0.03\,(\text{syst}) & \text{for } 0.045 < q^2 < 1.1 \;\; \text{GeV}^2/c^4 \\ 0.69 \,{}^{+\,0.11}_{-\,0.07}\,(\text{stat}) \pm 0.05\,(\text{syst}) & \text{for } 1.1 \;\; < q^2 < 6.0 \;\; \text{GeV}^2/c^4 \end{cases}$$

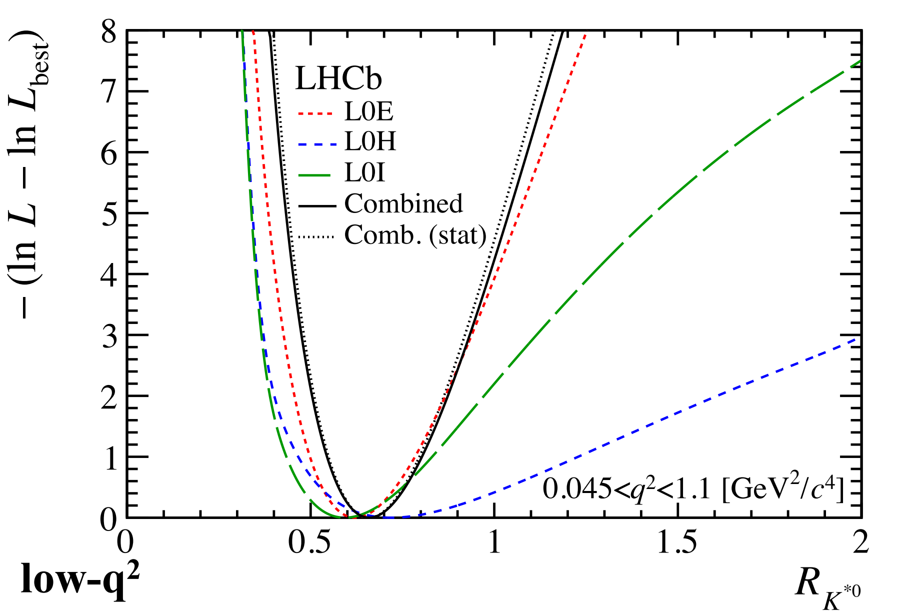

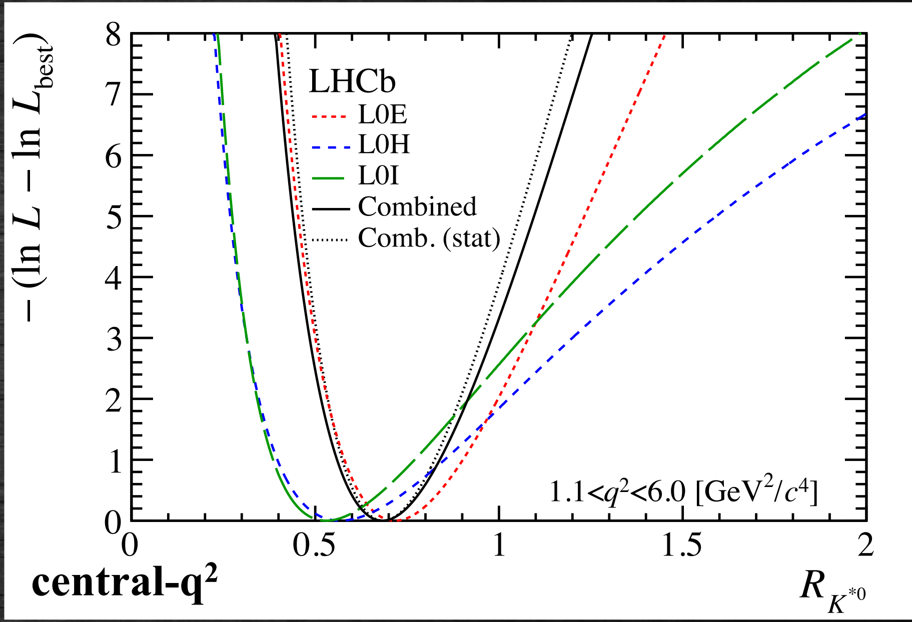

- The measured values of $R_{K^{*0}}$ are found to be in good agreement among the three trigger categories in both q^2 regions
- About half of the systematic uncertainty is correlated between the two q^2 regions

arXiv:1705.05802

Results – II

$$R_{K^{*0}} = \begin{cases} 0.66 \, ^{+\,0.11}_{-\,0.07} \,(\text{stat}) \pm 0.03 \,(\text{syst}) & \text{for } 0.045 < q^2 < 1.1 \;\; \text{GeV}^2/c^4 \\ 0.69 \, ^{+\,0.11}_{-\,0.07} \,(\text{stat}) \pm 0.05 \,(\text{syst}) & \text{for } 1.1 \;\; < q^2 < 6.0 \;\; \text{GeV}^2/c^4 \end{cases}$$

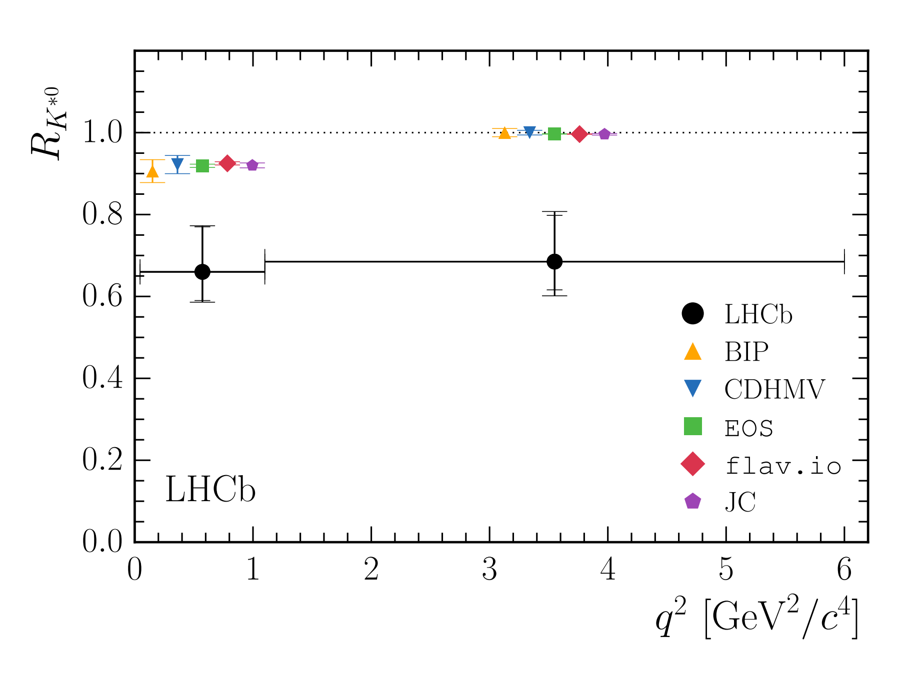

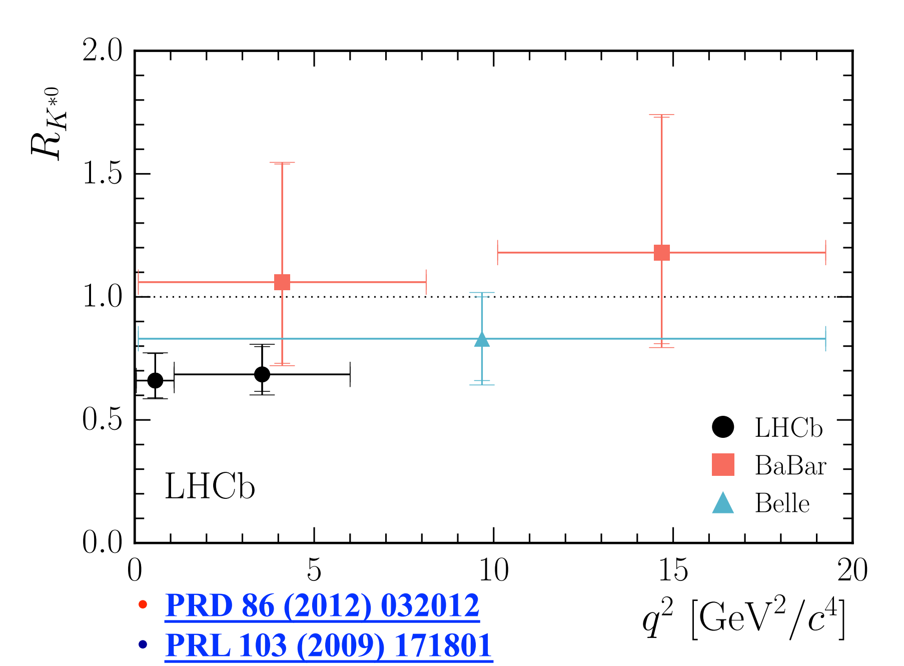

- PRD 86 (2012) 032012
- PRL 103 (2009) 171801

› Compatibility with the SM prediction(s)

» **low-q²** 2.1-2.3 standard deviations

» **central-q²** 2.4-2.5 standard deviations

arXiv:1705.05802

Global Fits – I

› Several attempts to interpret results by performing **global fits to data**

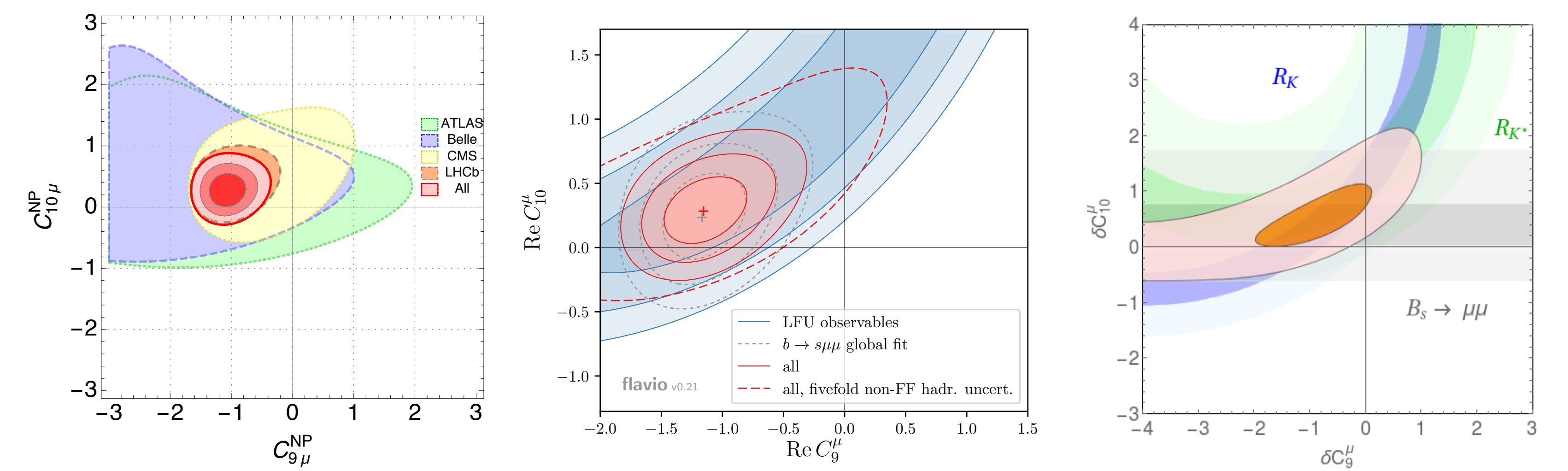

arXiv:1704.05340 arXiv:1704.05435 arXiv:1704.05446

› Take into account O(100) observables from different experiments, including B→μμ, b→sll and b→sγ transitions

› All global fits require an **additional contribution with respect to the SM to accommodate the data, with a preference for NP in C_9 at 3-5σ**

› **Or is this a problem with the understanding of QCD?**
e.g. correctly estimating the contribution from charm loops?

Global Fits – II

- **Good consistency among different fits**
  - BFs and Angular Observables
  - Different modes
  - Different q^2 regions

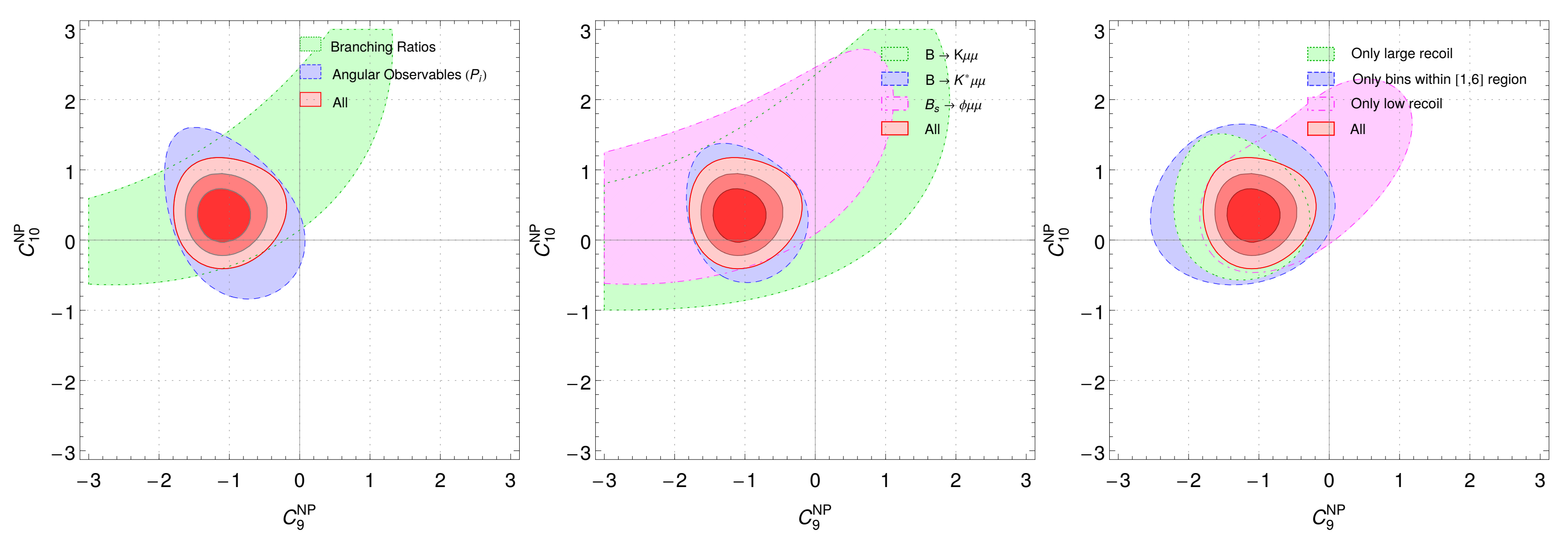

arXiv:1510.04239

- n.b. Different theory issues in each case

Is it a Z', a LQ or ... ?

- Models containing a **new heavy gauge boson** or **leptoquarks** have been proposed to explain the anomalies in the flavour sector

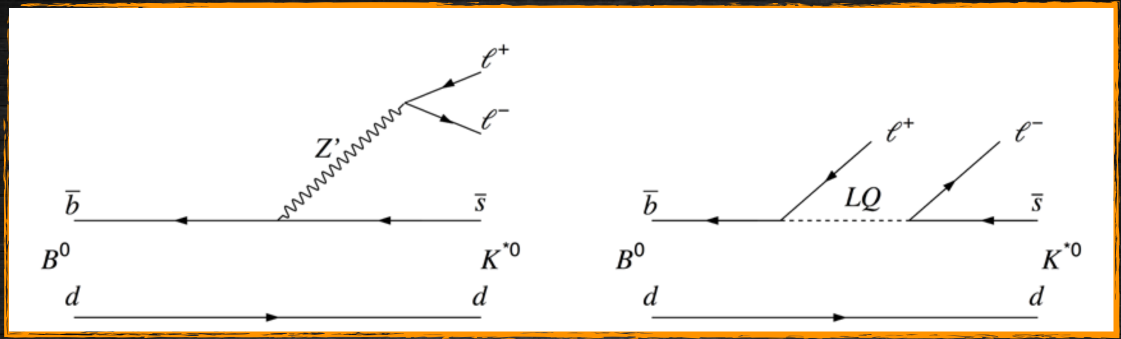

- e.g. Low energy scalar leptoquark

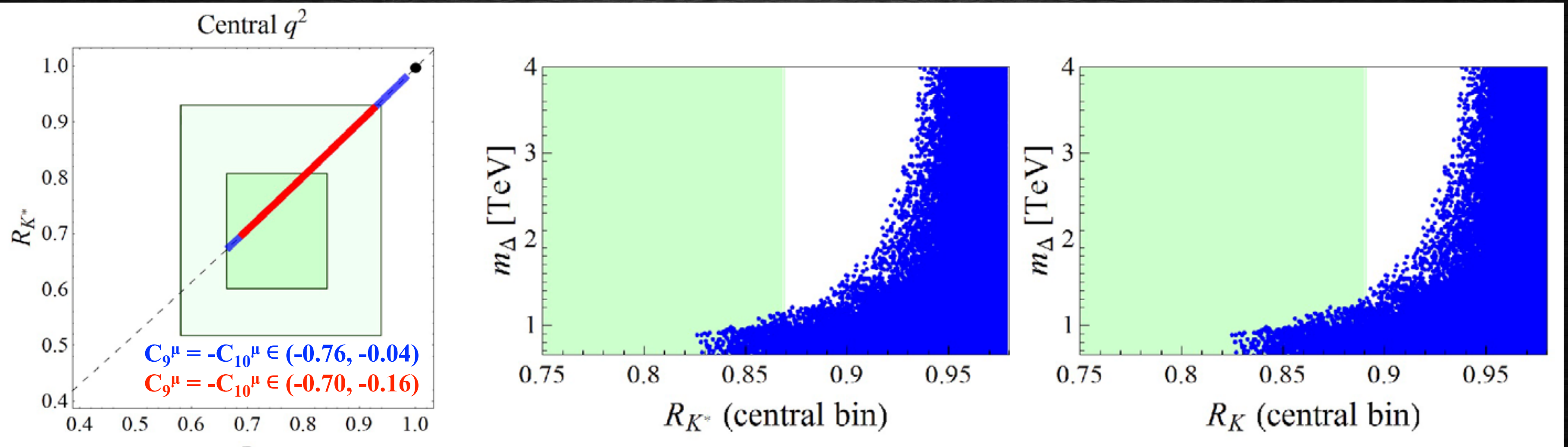

arXiv:1704.05835

Outlook – I

- **"Relatively soon" updates** to confirm any discrepancy independently of combination with BF and angular analyses

- **R_K**
  - » Improvements to offline processing
  - » 2015-2016 data (0.3+1.6 fb^{-1})
  - » Can expect stat error to go down by a factor ~1.8
  - » Add high-q^2

- **$R_{K^{*0}}$**
  - » 2015-2016 data (0.3+1.6 fb^{-1})
  - » Can expect stat error to go down by a factor ~1.5
  - » Add high-q^2

- **R_ϕ**
  - » Analogous measurement with $B_s \to \phi ll$
  - » Cons: signal suppression (f_s/f_d and BF=1/2)
  - » Pros: narrow ϕ mass and less part-reco background

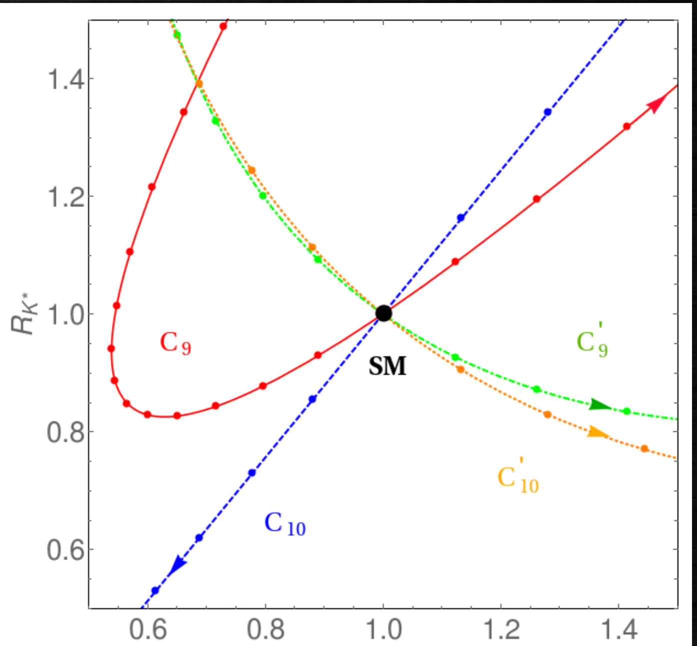

arXiv:1704.05446

Outlook – II

- Several **additional final states** under study
  - K_S
  - K^{*+}
  - Higher K^* resonances
  - $K\pi\pi$
  - pK

- Remainder of Run-II will add further ~2 fb^{-1}/year
  → Run-II total integrated luminosity ~6 fb^{-1}
- Twice cross-section in Run-II than Run-I
  → **Run-I + Run-II will effectively have ~5x statistics than Run-I**
- Analyses most likely to still be statistically dominated but will start to hit systematics in some areas

- More details can be found at [Instant workshop on B anomalies]()

Summary

- Using the full Run-I data set the $R_{K^{*0}}$ ratio has been measured by LHCb with the best precision to date in two q^2 bins
- The compatibility of the result with the SM prediction(s) is of 2.1-2.3 and 2.4-2.5 standard deviations in the two q^2 regions
- The result is particularly interesting given a similar behaviour in R_K and several other anomalies in the flavour sector
- Rare decays will largely benefit from the increase in energy and collected data of Run-II
- LHCb has a wide programme of LU tests based on similar ratios
- Future measurements will be able to clarify whether the tantalising hints we are observing are a glimpse of NP

Backup

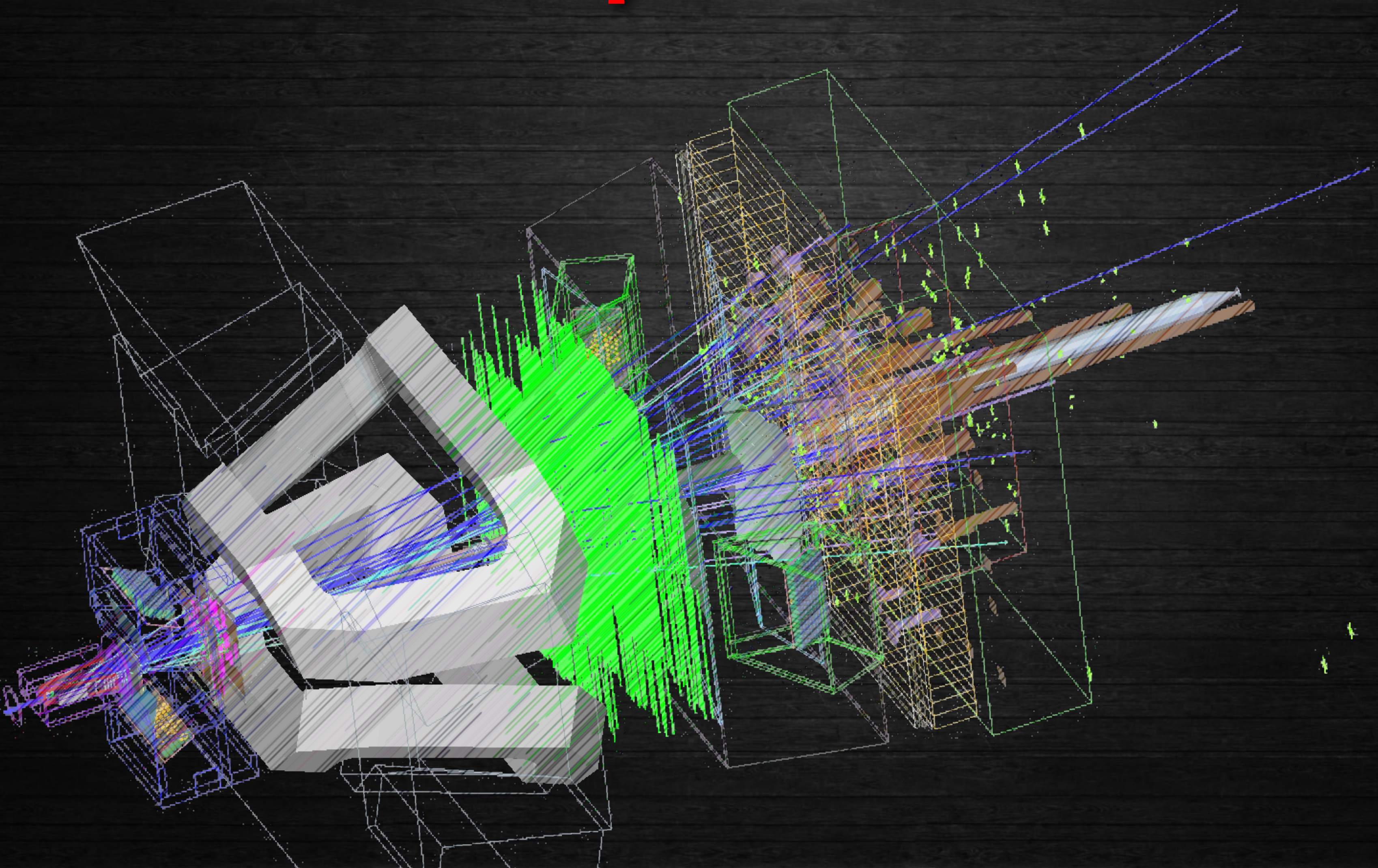

Calorimeter System

- Composed of a Scintillating Pad Detector (SPD), a Preshower (PS), an electromagnetic calorimeter (ECAL) and a hadronic calorimeter (HCAL)
- The SPD and the PS consist of a plane of scintillator tiles (2.5 radiation lengths, but to only ~6% hadronic interaction lengths)
- The ECAL has shashlik-type construction, i.e. a stack of alternating slices of lead absorber and scintillator (25 radiation lengths)
- The HCAL is a sampling device made from iron and scintillator tiles being orientated parallel to the beam axis (5.6 interaction lengths)

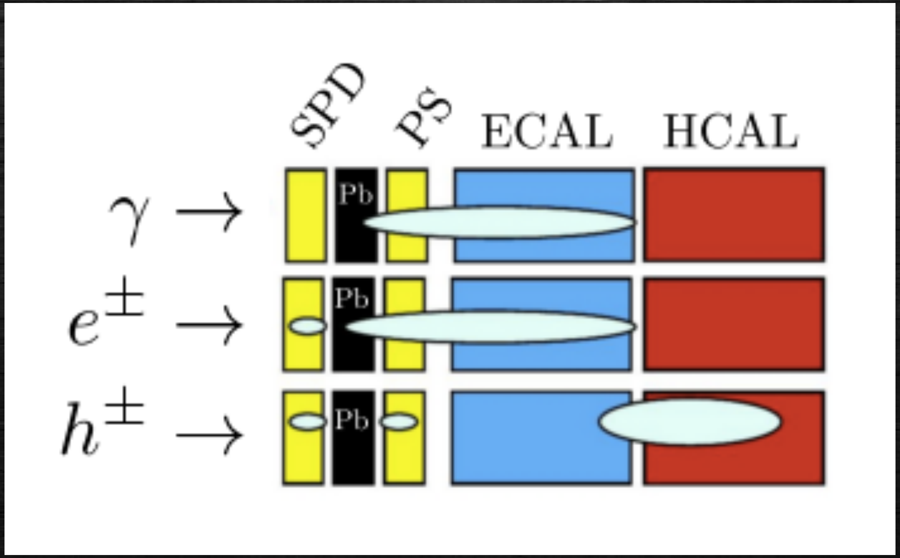

Test of LU – $R_{K^{*0}}$

› Test of LFU with **$B^0 \to K^{*0}\mu\mu$** and **$B^0 \to K^{*0}ee$**

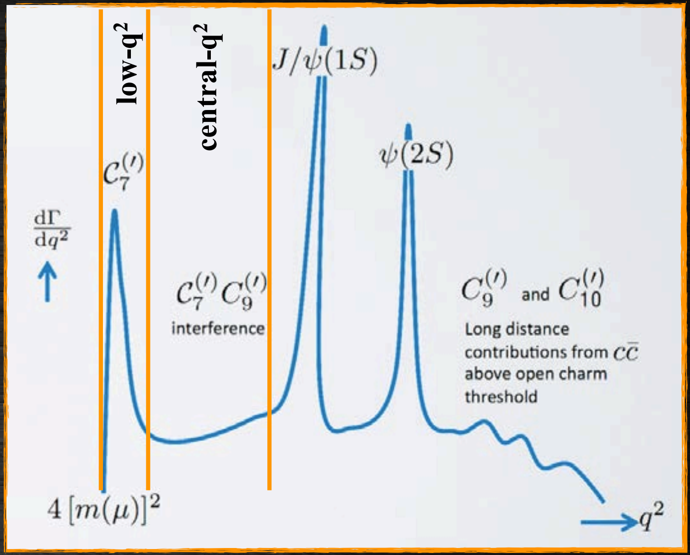

› **Two regions of q²**

» Low [0.045-1.1] GeV²/c⁴

» Central [1.1-6.0] GeV²/c⁴

› Measured relative to **$B^0 \to K^{*0}J/\psi(ll)$** in order to reduce systematics

$$\mathcal{R}_{K^{*0}} = \frac{\mathcal{B}(B^0 \to K^{*0}\mu^+\mu^-)}{\mathcal{B}(B^0 \to K^{*0}J/\psi(\to \mu^+\mu^-))} \Bigg/ \frac{\mathcal{B}(B^0 \to K^{*0}e^+e^-)}{\mathcal{B}(B^0 \to K^{*0}J/\psi(\to e^+e^-))}$$

› K^{*0} reconstructed as **$K^+\pi^-$** within 100MeV from the $K^*(892)^0$

› **Blind analysis** to avoid experimental biases

› Extremely challenging due to significant differences in the way muons and electrons "interact" with the detector (bremsstrahlung and trigger)

Fit Procedure – μμ

- Fit signal MC to extract initial parameters
- Simultaneous fit to resonant and non-resonant data allowing (some) parameters to vary

- **Signal**
  - Hypatia — [NIM A, 764, 150 (2014)]
  - Free parameters — mass shift and width scale

- **Backgrounds**
  - **Combinatorial** — exponential
  - **$\Lambda_b \to KpJ/\psi(\mu\mu)$** — simulation & data
  - **$B_s \to K^{*0}J/\psi(\mu\mu)$** — same as signal but shifted by m_{Bs}-m_{B0}

  (last two: $B^0 \to K^{*0}J/\psi$ only)

Fit Procedure – ee

- Fit signal MC to extract initial parameters
- Simultaneous fit to resonant and non-resonant data split in trigger categories allowing (some) parameters to vary (bremsstrahlung fractions fixed from MC)

- **Signal**
  - Crystal-Ball (Crystal-Ball and Gaussian)
  - Free parameters — mass shift and width scale

- **Backgrounds**
  - **Combinatorial** — exponential
  - **$\Lambda_b \to KpJ/\psi(ee)$** — simulation & data, constrained using muons
  - **$B_s \to K^{*0}J/\psi(ee)$** — same as signal but shifted by m_{Bs}-m_{B0}, constrained using muons

  (Λ_b and B_s backgrounds: $B^0 \to K^{*0}J/\psi$ only)

  - **$B^0 \to K^{*0}J/\psi$ Leakage** — simulation, yield constrained using data
  - **Part-Reco** — simulation & data

  (Leakage and Part-Reco: $B^0 \to K^{*0}ee$ only)

Yields

› Precision of the measurement driven by the statistics of the electron samples

	$B^0 \to K^{*0}\ell^+\ell^-$		$B^0 \to K^{*0} J/\psi (\to \ell^+\ell^-)$
	low-q^2	central-q^2	
$\mu^+\mu^-$	$285\ ^{+\ 18}_{-\ 18}$	$353\ ^{+\ 21}_{-\ 21}$	$274416\ ^{+\ 602}_{-\ 654}$
e^+e^- (L0E)	$55\ ^{+\ 9}_{-\ 8}$	$67\ ^{+\ 10}_{-\ 10}$	$43468\ ^{+\ 222}_{-\ 221}$
e^+e^- (L0H)	$13\ ^{+\ 5}_{-\ 5}$	$19\ ^{+\ 6}_{-\ 5}$	$3388\ ^{+\ 62}_{-\ 61}$
e^+e^- (L0I)	$21\ ^{+\ 5}_{-\ 4}$	$25\ ^{+\ 7}_{-\ 6}$	$11505\ ^{+\ 115}_{-\ 114}$

› In total, about 90 and 110 $B^0 \to K^{*0}ee$ candidates at low- and central-q^2, respectively

Cross-Checks – I

› **Control of the absolute scale of the efficiencies** via the ratio

$$r_{J/\psi} = \frac{\mathcal{B}(B^0 \to K^{*0} J/\psi(\to \mu^+\mu^-))}{\mathcal{B}(B^0 \to K^{*0} J/\psi(\to e^+e^-))}$$

which is expected to be unity and measured to be

$$1.043 \pm 0.006\,(\mathrm{stat}) \pm 0.045\,(\mathrm{syst})$$

› Result observed to be independent of the decay kinematics and event multiplicity

› Extremely stringent test, which does not benefit from the cancellation of the experimental systematics provided by the double ratio

Cross-Checks – II

- **BR($B^0 \to K^{*0}\mu\mu$)** in good agreement with [arXiv:1606.04731]

- If **corrections to simulations** are not accounted for, the ratio of the efficiencies changes by less than 5%

- **Further checks** performed by measuring the following ratios

$$\mathcal{R}_{\psi(2S)} = \frac{\mathcal{B}(B^0 \to K^{*0}\psi(2S)(\to \mu^+\mu^-))}{\mathcal{B}(B^0 \to K^{*0}J/\psi(\to \mu^+\mu^-))} \Bigg/ \frac{\mathcal{B}(B^0 \to K^{*0}\psi(2S)(\to e^+e^-))}{\mathcal{B}(B^0 \to K^{*0}J/\psi(\to e^+e^-))}$$

$$r_\gamma = \frac{\mathcal{B}(B^0 \to K^{*0}\gamma(\to e^+e^-))}{\mathcal{B}(B^0 \to K^{*0}J/\psi(\to e^+e^-))}$$

which are found to be compatible with the expectations

Cross-Checks – III

› Relative population of **bremsstrahlung categories** compared between data and simulation using $B^0 \to K^{*0} J/\psi(ee)$ and $B^0 \to K^{*0}\gamma(ee)$ events

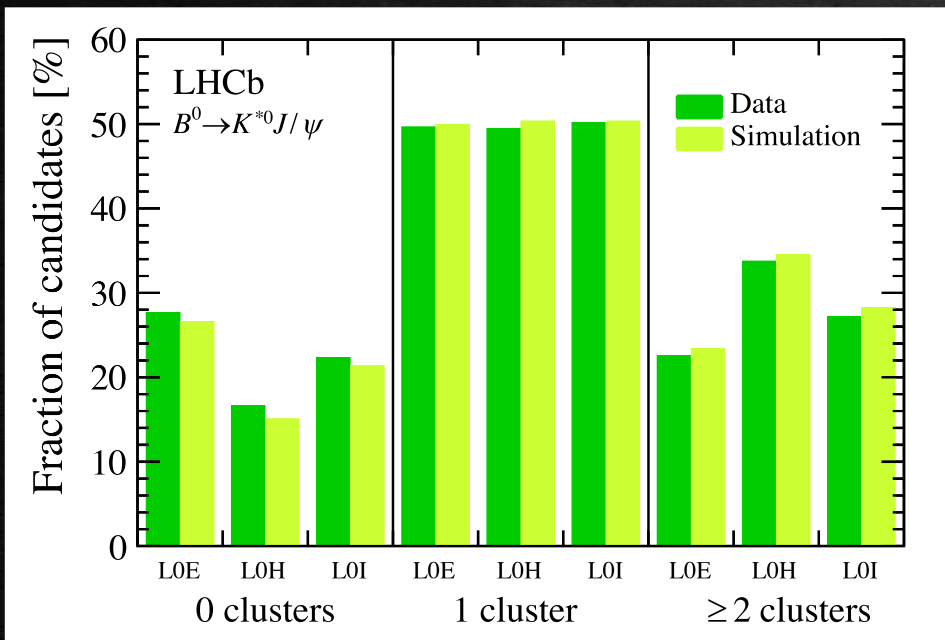

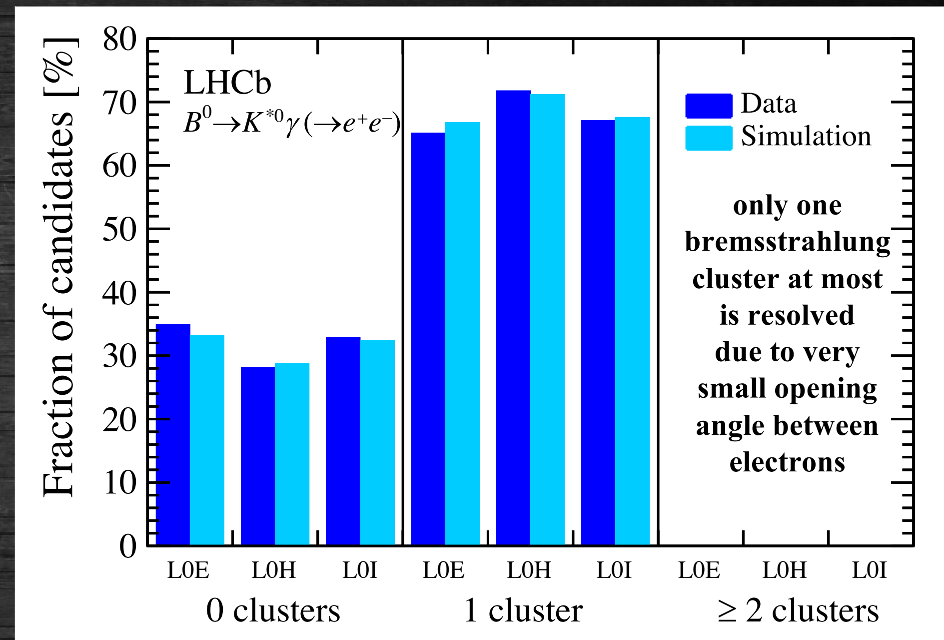

› A good agreement is observed

Cross-Checks – IV

› The sPlot technique is used to statistically subtract the background from the selected data [NIM A555, 356-369 (2005)]

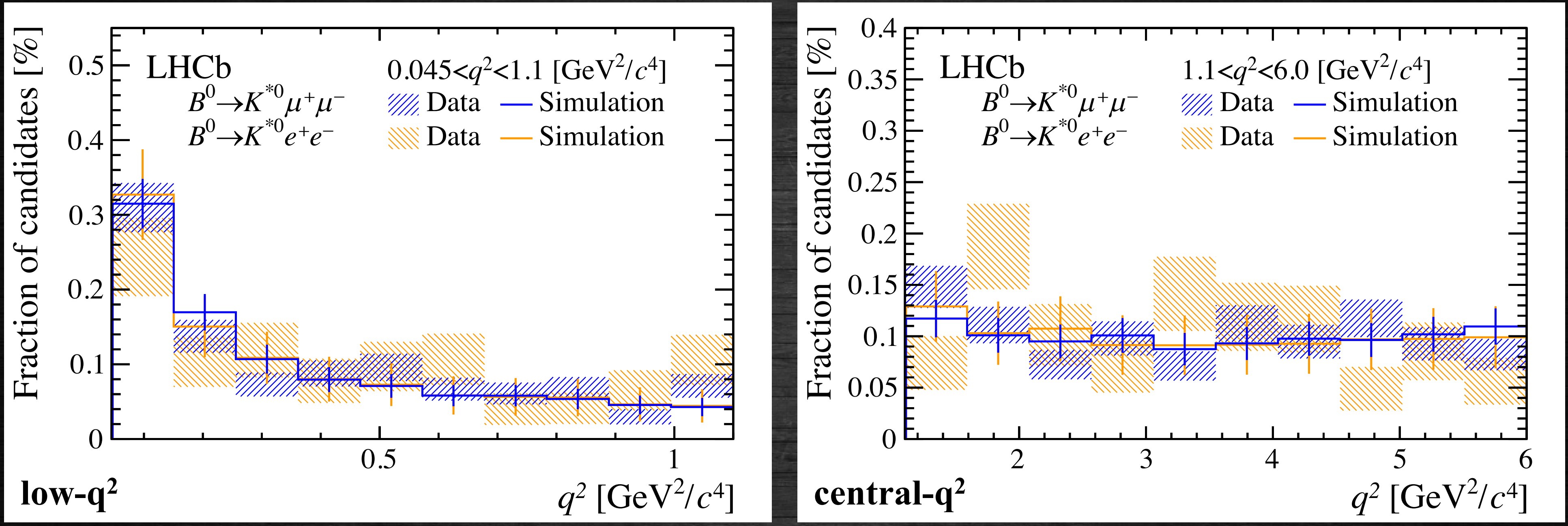

› A good agreement is observed in both q^2 regions between muons and electrons, data and simulation

Cross-Checks – V

- No attempt is made to separate the K^{*0} meson from S-wave or other broad contributions present in the mass peak region

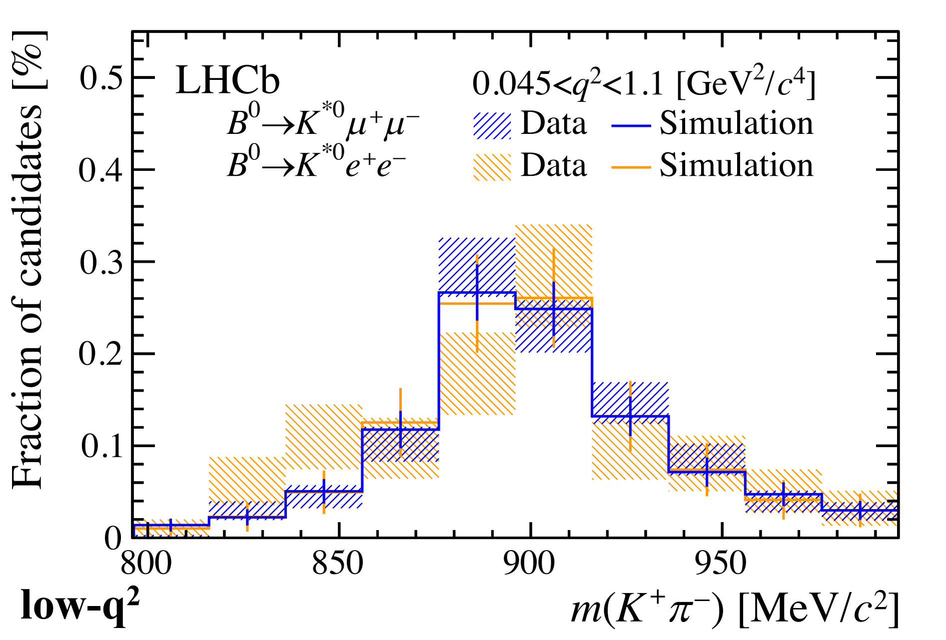

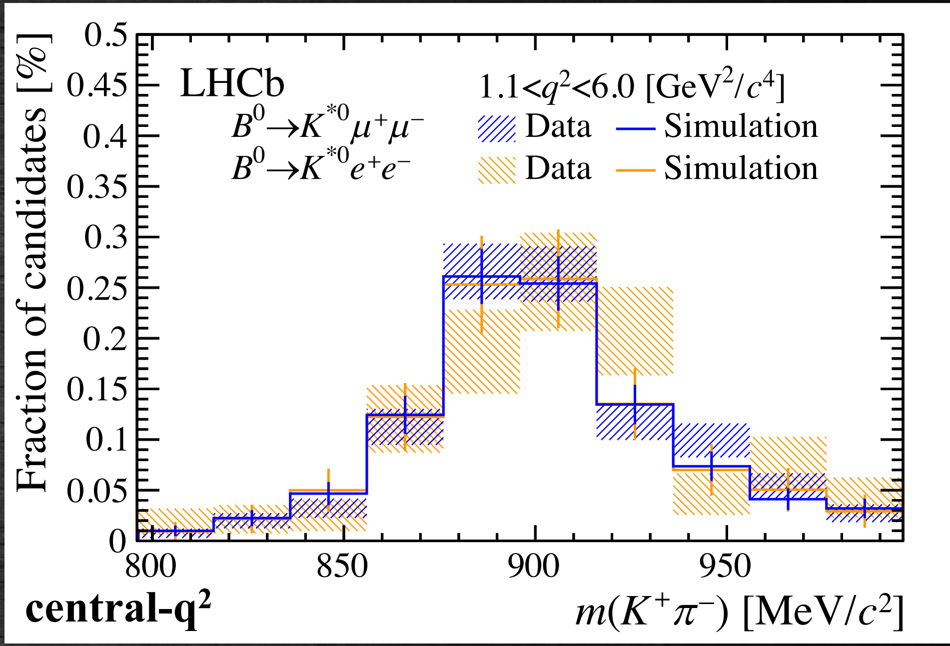

- A clear K^{*0} mass peak is visible, and the muon and electron channels manifest a very good agreement

Cross-Checks – VI

› The opening angle between the two leptons

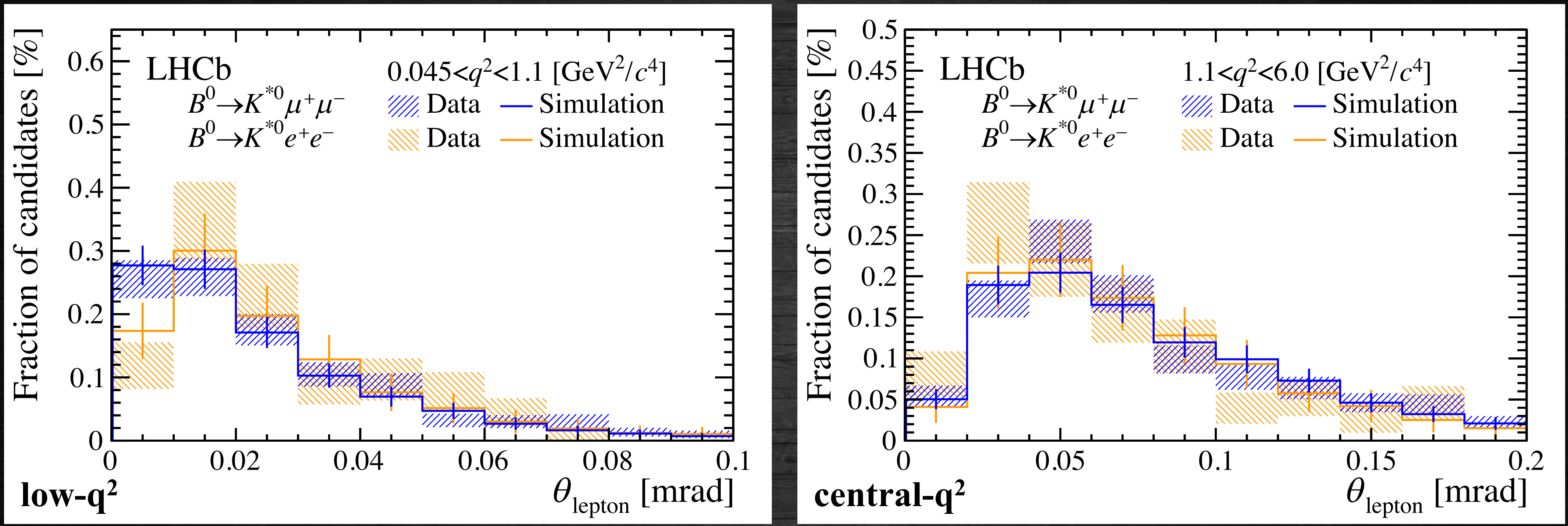

› The distribution is different between muons and electrons at low-q^2 because of the difference in the lepton masses

Cross-Checks – VII

› The distance between the Kπ and ll vertices

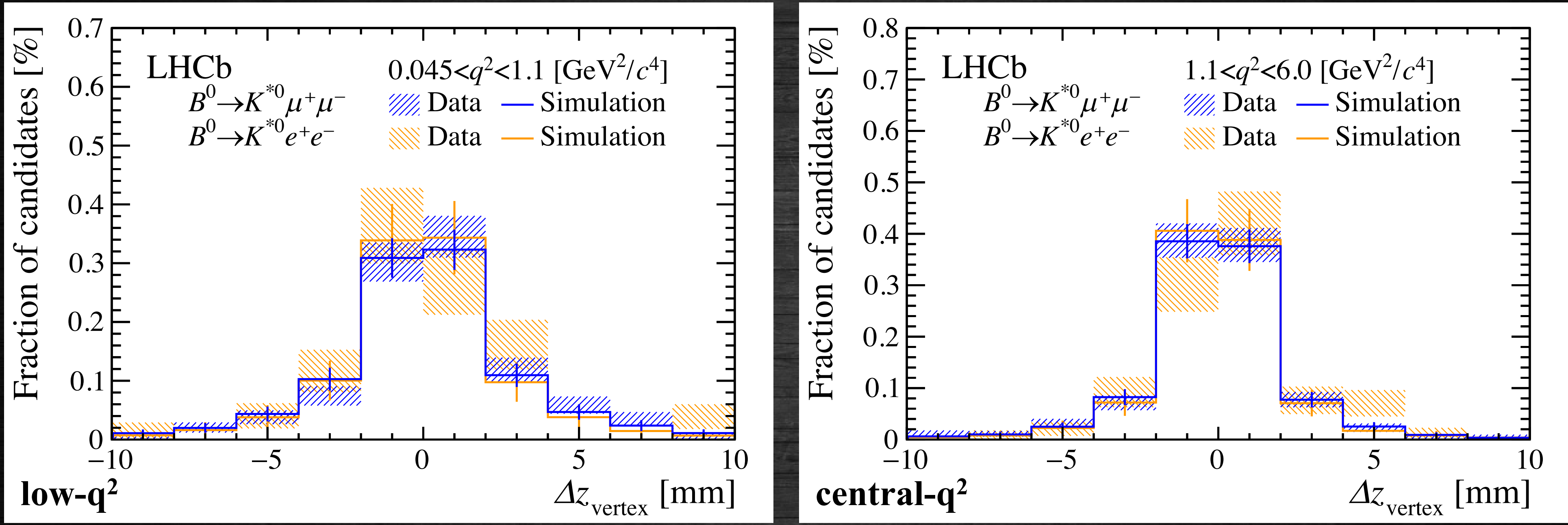

› The hadron and lepton pairs consistently originate from the same decay vertex

Systematics

- $R_{K^{*0}}$ **determined as a double ratio**
  - Many experimental systematic effects cancel
  - Statistically dominated (~15%)

arXiv:1705.05802

	$\Delta R_{K^{*0}}/R_{K^{*0}}$ [%]					
	low-q^2			central-q^2		
Trigger category	L0E	L0H	L0I	L0E	L0H	L0I
Corrections to simulation	2.5	4.8	3.9	2.2	4.2	3.4
Trigger	0.1	1.2	0.1	0.2	0.8	0.2
PID	0.2	0.4	0.3	0.2	1.0	0.5
Kinematic selection	2.1	2.1	2.1	2.1	2.1	2.1
Residual background	–	–	–	5.0	5.0	5.0
Mass fits	1.4	2.1	2.5	2.0	0.9	1.0
Bin migration	1.0	1.0	1.0	1.6	1.6	1.6
$r_{J/\psi}$ ratio	1.6	1.4	1.7	0.7	2.1	0.7
Total	4.0	6.1	5.5	6.4	7.5	6.7

← Description of brem-tail

← Residual background contamination due to $B^0 \to K^{*0} J/\psi(ee)$ with a $K \leftrightarrow e$ or $\pi \leftrightarrow e$ swap

- Total systematic uncertainty of 4-6% and 6-8% at low- and central-q^2

Systematics – III

› **Mass fit**: a systematic uncertainty is determined by running pseudo-experiments with different descriptions of the signal and background fit models

› **Bin migration**: the effect of the model dependence and description of the q^2 resolution in simulation are assigned as a systematic uncertainty

› **$r_{J/\psi}$ ratio**: the ratio is studied as a function of several properties of the event and decay products, and the observed residual deviations from unity are used to assign a systematic uncertainty

arXiv:1705.05802

	$\Delta R_{K^{*0}}/R_{K^{*0}}$ [%]					
	low-q^2			central-q^2		
Trigger category	L0E	L0H	L0I	L0E	L0H	L0I
Corrections to simulation	2.5	4.8	3.9	2.2	4.2	3.4
Trigger	0.1	1.2	0.1	0.2	0.8	0.2
PID	0.2	0.4	0.3	0.2	1.0	0.5
Kinematic selection	2.1	2.1	2.1	2.1	2.1	2.1
Residual background	–	–	–	5.0	5.0	5.0
Mass fits	1.4	2.1	2.5	2.0	0.9	1.0
Bin migration	1.0	1.0	1.0	1.6	1.6	1.6
$r_{J/\psi}$ ratio	1.6	1.4	1.7	0.7	2.1	0.7
Total	4.0	6.1	5.5	6.4	7.5	6.7

	$\varepsilon_{\ell^+\ell^-}/\varepsilon_{J/\psi\,(\ell^+\ell^-)}$	
	low-q^2	central-q^2
$\mu^+\mu^-$	0.679 ± 0.009	0.584 ± 0.006
e^+e^- (L0E)	0.539 ± 0.013	0.522 ± 0.010
e^+e^- (L0H)	2.252 ± 0.098	1.627 ± 0.066
e^+e^- (L0I)	0.789 ± 0.029	0.595 ± 0.020

References

q^2 range $[\,\mathrm{GeV}^2/c^4\,]$	$R_{K^{*0}}^{\mathrm{SM}}$	References
$[0.045, 1.1]$	0.906 ± 0.028	BIP [26]
	0.922 ± 0.022	CDHMV [27–29]
	$0.919\,^{+0.004}_{-0.003}$	EOS [30, 31]
	0.925 ± 0.004	flav.io [32–34]
	$0.920\,^{+0.007}_{-0.006}$	JC [35]
$[1.1, 6.0]$	1.000 ± 0.010	BIP [26]
	1.000 ± 0.006	CDHMV [27–29]
	$0.9968\,^{+0.0005}_{-0.0004}$	EOS [30, 31]
	0.9964 ± 0.005	flav.io [32–34]
	0.996 ± 0.002	JC [35]

References

[26] M. Bordone, G. Isidori, and A. Pattori, *On the Standard Model predictions for R_K and R_{K^*}*, Eur. Phys. J. **C76** (2016) 440, arXiv:1605.07633.

[27] S. Descotes-Genon, L. Hofer, J. Matias, and J. Virto, *Global analysis of $b \to s\ell\ell$ anomalies*, JHEP **06** (2016) 092, arXiv:1510.04239.

[28] B. Capdevila, S. Descotes-Genon, J. Matias, and J. Virto, *Assessing lepton-flavour non-universality from $B \to K^*\ell\ell$ angular analyses*, JHEP **10** (2016) 075, arXiv:1605.03156.

[29] B. Capdevila, S. Descotes-Genon, L. Hofer, and J. Matias, *Hadronic uncertainties in $B \to K^*\mu^+\mu^-$: a state-of-the-art analysis*, JHEP **04** (2017) 016, arXiv:1701.08672.

[30] N. Serra, R. Silva Coutinho, and D. van Dyk, *Measuring the breaking of lepton flavour universality in $B \to K^*\ell^+\ell^-$*, Phys. Rev. **D95** (2017) 035029, arXiv:1610.08761.

[31] D. van Dyk *et al.*, *EOS — A HEP program for flavor observables*, https://eos.github.io; D. van Dyk *et al.*, *EOS ("delta456" release)*, doi: 10.5281/zenodo.159680.

[32] A. Bharucha, D. M. Straub, and R. Zwicky, *$B \to V\ell^+\ell^-$ in the Standard Model from light-cone sum rules*, JHEP **08** (2016) 098, arXiv:1503.05534.

[33] W. Altmannshofer, C. Niehoff, P. Stangl, and D. M. Straub, *Status of the $B \to K^*\mu^+\mu^-$ anomaly after Moriond 2017*, arXiv:1703.09189.

[34] D. Straub *et al.*, *flav-io/flavio v0.19*, doi: 10.5281/zenodo.292991.

[35] S. Jäger and J. Martin Camalich, *Reassessing the discovery potential of the $B \to K^*\ell^+\ell^-$ decays in the large-recoil region: SM challenges and BSM opportunities*, Phys. Rev. **D93** (2016) 014028, arXiv:1412.3183.

› What about NP?

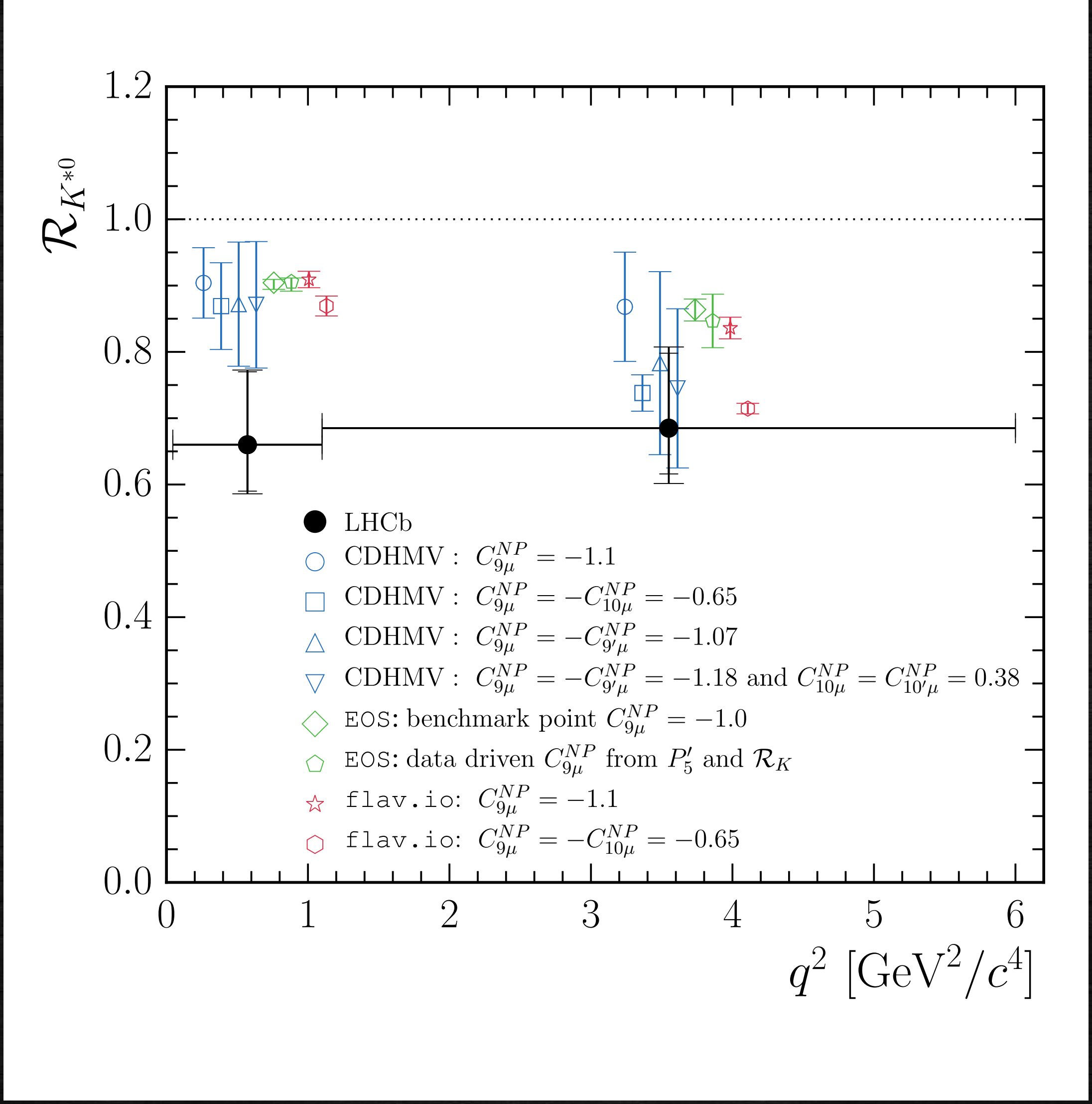

Muon Reconstruction

- **Extremely performant in LHCb**:
  - dedicated muon chambers
  - very efficient tracking system.
- **A muon is a clear trigger signature**:
  ε(L0+HLT)= ~90% for di-muon channels
  ε(L0+HLT)= ~30% for multibody hadronic states
- **Very good di-muon resolution**

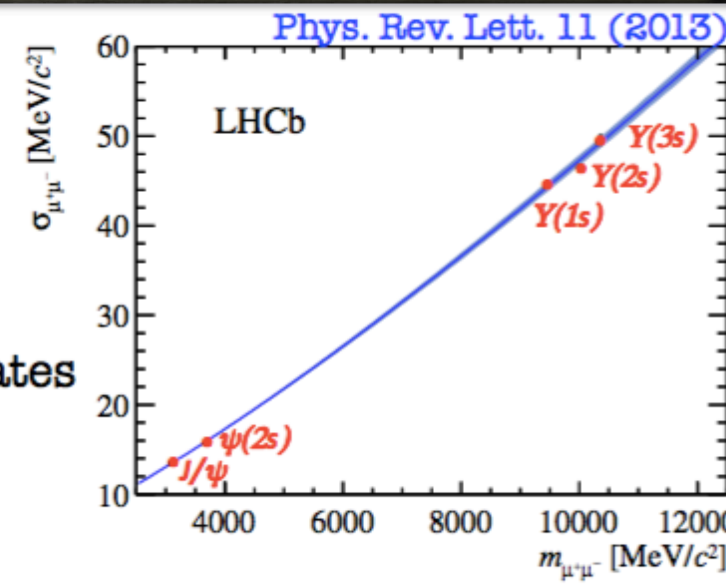

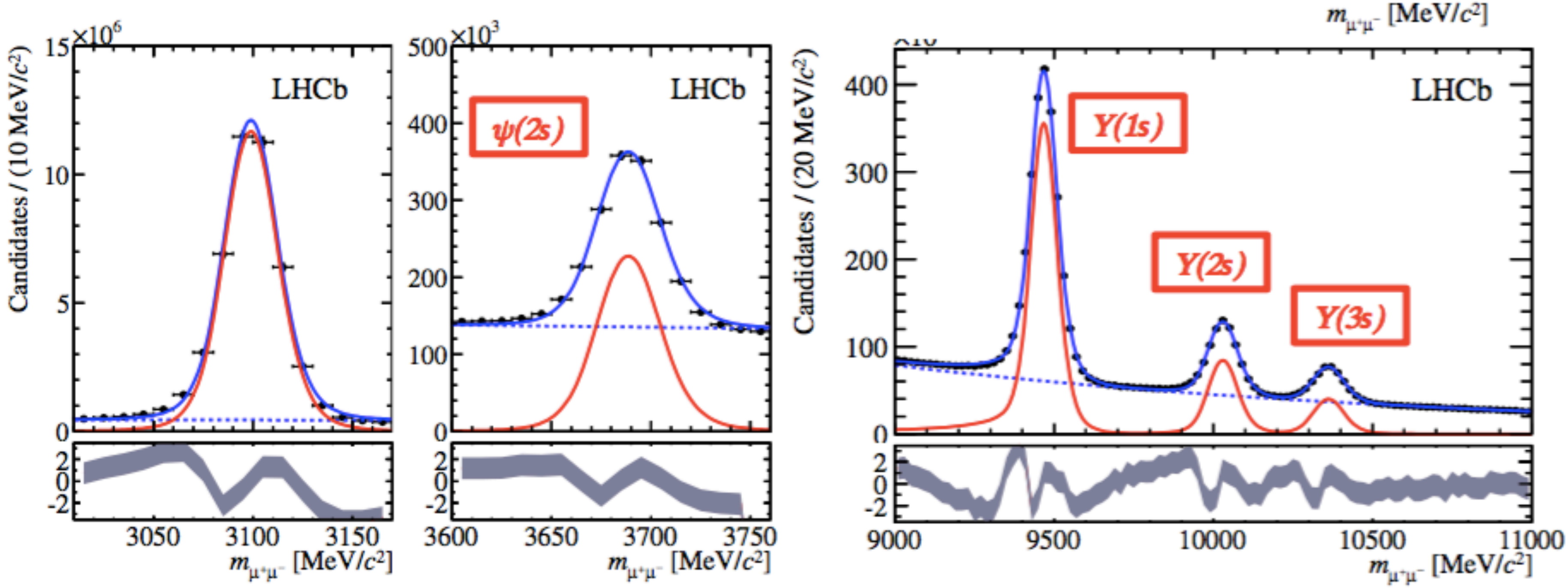

Effective Theory Approach

$$H_{eff} = -\frac{4G_F}{\sqrt{2}} V_{tb} V_{ts}^{*} \sum_i \Big[\underbrace{C_i(\mu) O_i(\mu)}_{\text{left-handed part}} + \underbrace{C'_i(\mu) O'_i(\mu)}_{\substack{\text{right-handed part} \\ \text{suppressed in SM}}} \Big]$$

i = 1, 2	Tree
i = 3 -6, 8	Gluon penguin
i = 7	Photon penguin
i = 9, 10	Electroweak penguin
i = S	Higgs (scalar) penguin
i = P	Pseudoscalar penguin

Operators O_i: non-perturbative long-distance effects

Wilson coefficients C_i: perturbative short-distance effects

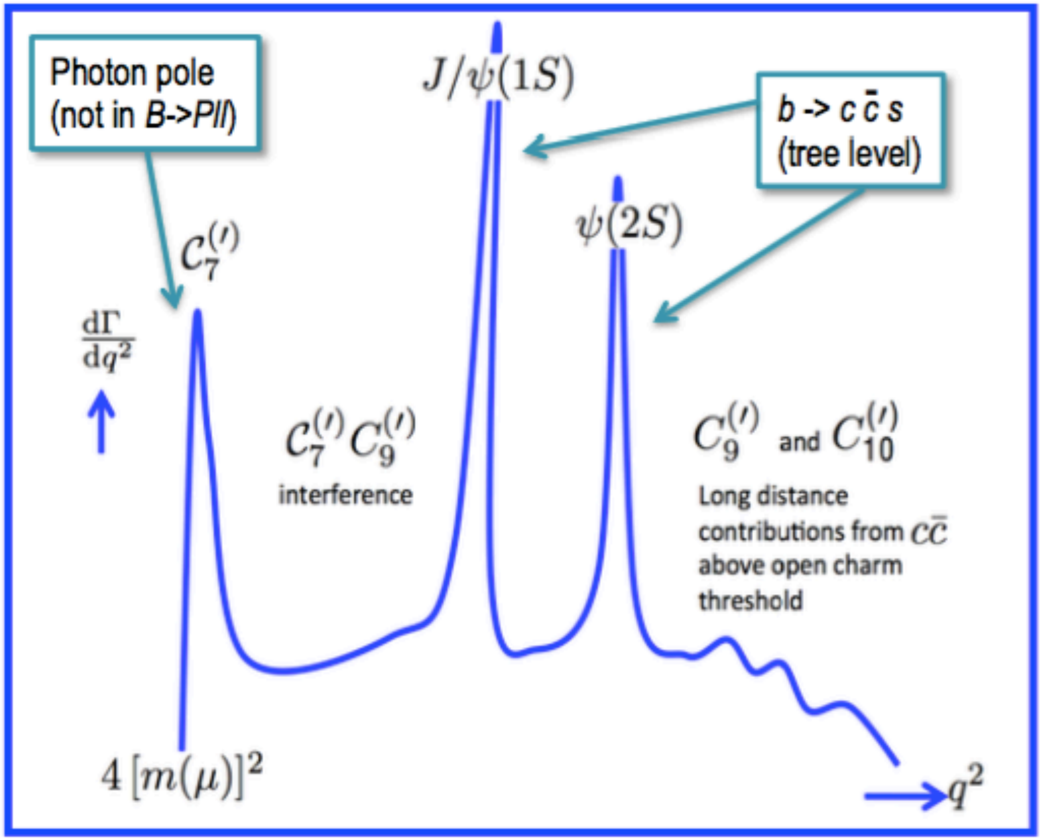

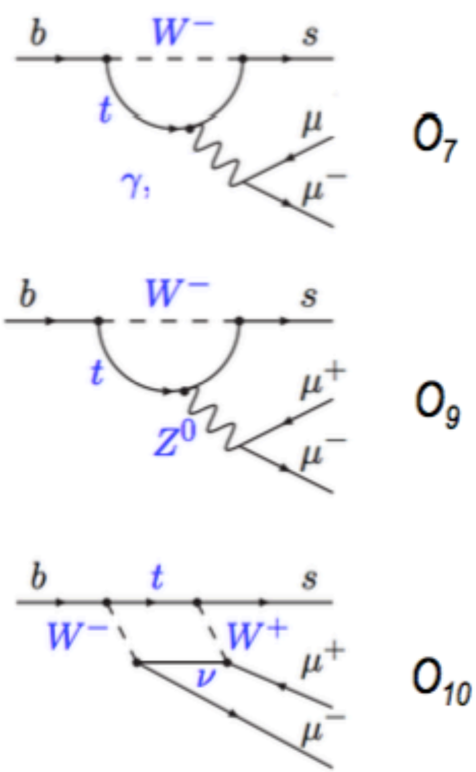

Sensitivity to Wilson Coefficients

- Different observables are complementary in constraining NP
- Leptonic decay uniquely sensitive to scalar operators

Decay	$C_7^{(\prime)}$	$C_9^{(\prime)}$	$C_{10}^{(\prime)}$	$C_{S,P}^{(\prime)}$
$B \to X_s \gamma$	X			
$B \to K^* \gamma$	X			
$B \to X_s \ell^+ \ell^-$	X	X	X	
$B \to K^{(*)} \ell^+ \ell^-$	X	X	X	
$B_s \to \mu^+ \mu^-$			X	X

Phase difference in $B^+ \to K^+\mu^+\mu^-$ decays

- Fit of to full dimuon mass distribution
  - Sum of relativistic Breit–Wigner amplitudes to describe resonances
  - short-distance contribution in terms of an effective field theory description
  - $B^+ \to J/\psi(\to \mu^+\mu^-)K^+$ as normalisation channel
- Magnitudes and relative phases between the resonances and the short-distance contribution allowed to vary in the fit
- Model includes: resonances (ρ, ω, ϕ, J/ψ, ψ(2S)) , charmonium states: (ψ(3770), ψ(4040), ψ(4160), ψ(4415))

[Eur. Phys. J. C (2017) 77: 161]

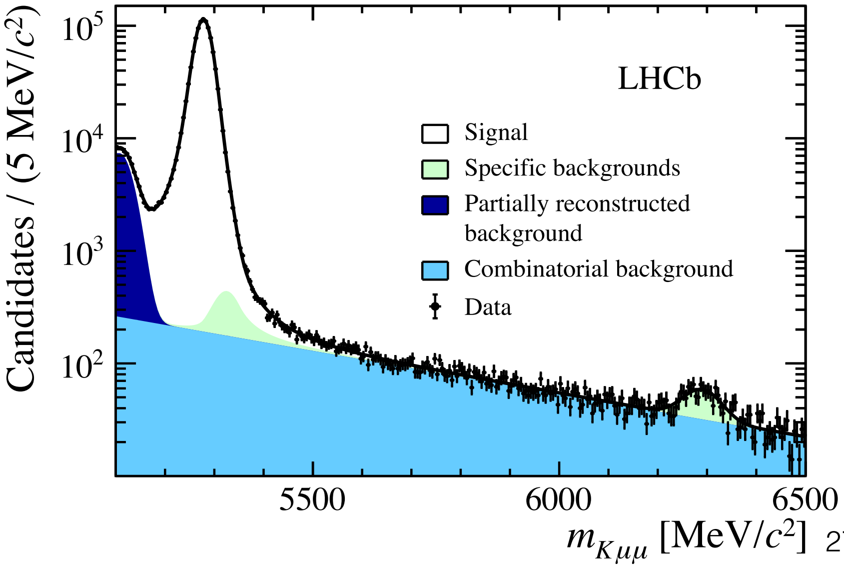

27

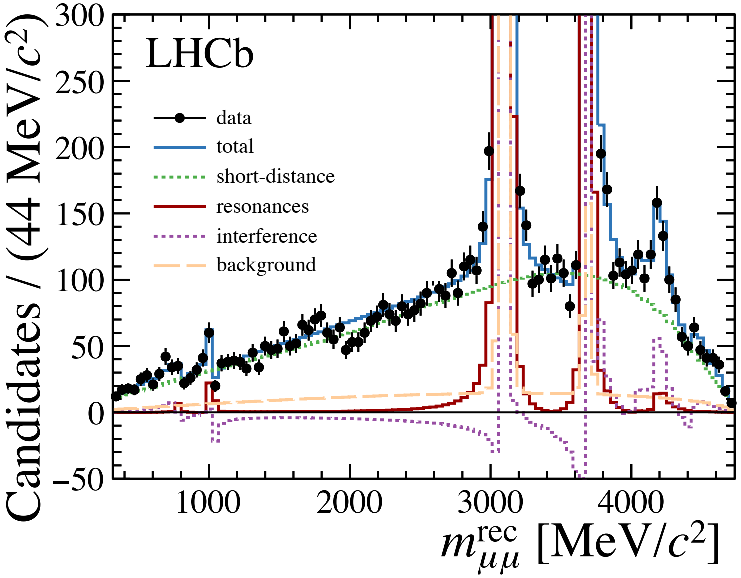

[Eur. Phys. J. C (2017) 77: 161]

Sensitive to C_9 and C_{10}:

$$\frac{\mathrm{d}\Gamma}{\mathrm{d}q^2} = \frac{G_F^2\alpha^2|V_{tb}V_{ts}^*|^2}{128\pi^5}|\boldsymbol{k}|\beta\left\{\frac{2}{3}|\boldsymbol{k}|^2\beta^2\left|\mathcal{C}_{10}f_+(q^2)\right|^2 + \frac{4m_\mu^2(m_B^2-m_K^2)^2}{q^2m_B^2}\left|\mathcal{C}_{10}f_0(q^2)\right|^2 + |\boldsymbol{k}|^2\left[1-\frac{1}{3}\beta^2\right]\left|\mathcal{C}_9 f_+(q^2) + 2\mathcal{C}_7\frac{m_b+m_s}{m_B+m_K}f_T(q^2)\right|^2\right\}$$

BF of the short-distance component:

$$\mathcal{B}(B^+\to K^+\mu^+\mu^-) = (4.37\pm0.15\pm0.23)\times10^{-7}$$

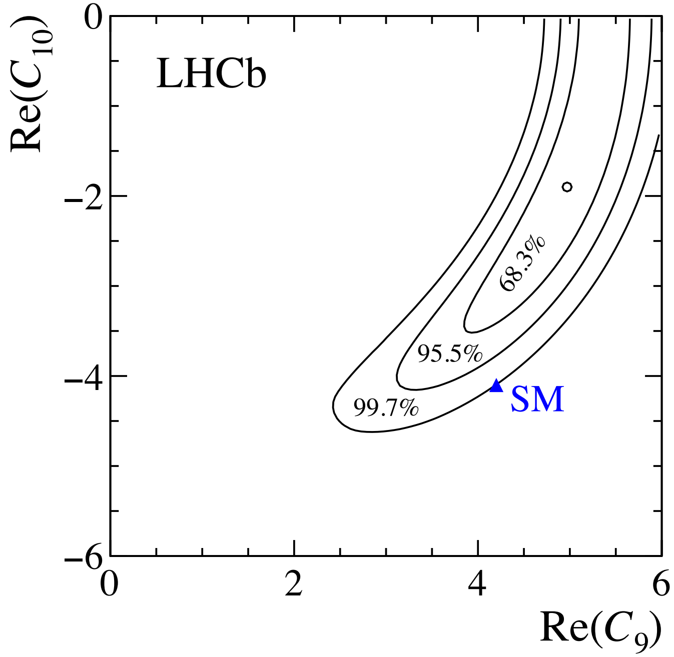

In very good agreement with the old result
[JHEP 06 (2014) 133]

Measurement of the Wilson coefficient:

- $|C_{10}| < |C_{10}^{SM}|$ and $|C_9| > |C_9^{SM}|$ if both free
- $|C_9| < |C_9^{SM}|$ if C_{10} constrained to the SM

Exclusion of C9 = 0 hypothesis > 5 σ

Compatible with previous measurement

Working on measurement in $B^0\to K^{*0}\mu^+\mu^-$

28

Angular Analyses

- Complex angular distribution:

$$\frac{1}{\mathrm{d}(\Gamma+\bar{\Gamma})/\mathrm{d}q^2}\frac{\mathrm{d}^3(\Gamma+\bar{\Gamma})}{\mathrm{d}\vec{\Omega}}\bigg|_{\mathrm{P}} = \frac{9}{32\pi}\Big[\tfrac{3}{4}(1-F_{\mathrm{L}})\sin^2\theta_K + F_{\mathrm{L}}\cos^2\theta_K +$$
$$+\tfrac{1}{4}(1-F_{\mathrm{L}})\sin^2\theta_K\cos 2\theta_l$$
$$-F_{\mathrm{L}}\cos^2\theta_K\cos 2\theta_l + S_3\sin^2\theta_K\sin^2\theta_l\cos 2\phi$$
$$+S_4\sin 2\theta_K\sin 2\theta_l\cos\phi + S_5\sin 2\theta_K\sin\theta_l\cos\phi$$
$$+\tfrac{4}{3}A_{\mathrm{FB}}\sin^2\theta_K\cos\theta_l + S_7\sin 2\theta_K\sin\theta_l\sin\phi$$
$$+S_8\sin 2\theta_K\sin 2\theta_l\sin\phi + S_9\sin^2\theta_K\sin^2\theta_l\sin 2\phi\Big]$$

fraction of longitudinal polarisation of the K*

forward-backward asymmetry of the dilepton system

The observables depend on form-factors for the $B \to K^*$ transition plus the underlying short distance physics (Wilson coefficients).